Identifying the causes and consequences of assembly gaps using a multiplatform genome assembly of a bird-of-paradise

Valentina Peona[1,2], Mozes P.K. Blom[3,4], Luohao Xu[5,6], Reto Burri[7], Shawn Sullivan[8], Ignas Bunikis[9], Ivan Liachko[8], Knud A. Jønsson[10], Qi Zhou[5,6,11], Martin Irestedt[3], Alexander Suh[1,2]

Affiliation

[1] Department of Ecology and Genetics – Evolutionary Biology, Uppsala University, Science for Life Laboratories, Norbyvägen 18D, SE-752 36, Uppsala, Sweden
[2] Department of Organismal Biology – Systematic Biology, Uppsala University, Norbyvägen 18D, SE-752 36, Uppsala, Sweden
[3] Department of Bioinformatics and Genetics, Swedish Museum of Natural History, SE-104 05, Stockholm, Sweden
[4] Museum für Naturkunde, Leibniz Institut für Evolutions- und Biodiversitätsforschung, Berlin, Germany
[5] MOE Laboratory of Biosystems Homeostasis & Protection, Life Sciences Institute, Zhejiang University, Hangzhou, China
[6] Department of Molecular Evolution and Development, University of Vienna, Vienna, Austria
[7] Department of Population Ecology, Institute of Ecology and Evolution, Friedrich-Schiller-University Jena, Dornburger Strasse 159, D-07743 Jena, Germany
[8] Phase Genomics, Inc. 1617 8th Ave N, Seattle, WA 98109 USA
[9] Uppsala Genome Center, Science for Life Laboratory, Dept. of Immunology, Genetics and Pathology, Uppsala University, SE‑752 37, Uppsala, Sweden
[10] Natural History Museum of Denmark, University of Copenhagen, Universitetsparken 15, DK-2100 Copenhagen, Denmark
[11] Center for Reproductive Medicine, The 2nd Affiliated Hospital, School of Medicine, Zhejiang University

Correspondence

V.P. (valentina.peona@ebc.uu.se), A.S. (alexander.suh@ebc.uu.se)

Keywords
Genome assembly, long reads, chromosome-level assembly, bird, transposable element, satellite repeat, GC content

Abstract

Genome assemblies are currently being produced at an impressive rate by consortia and individual laboratories. The low costs and increasing efficiency of sequencing technologies have opened up a whole new world of genomic biodiversity. Although these technologies generate high-quality genome assemblies, there are still genomic regions difficult to assemble, like repetitive elements and GC-rich regions (genomic "dark matter"). In this study, we compare the efficiency of currently used

sequencing technologies (short/linked/long reads and proximity ligation maps) and combinations thereof in assembling genomic dark matter starting from the same sample. By adopting different *de-novo* assembly strategies, we were able to compare each individual draft assembly to a curated multiplatform one and identify the nature of the previously missing dark matter with a particular focus on transposable elements, multi-copy MHC genes, and GC-rich regions. Thanks to this multiplatform approach, we demonstrate the feasibility of producing a high-quality chromosome-level assembly for a non-model organism (paradise crow) for which only suboptimal samples are available. Our approach was able to reconstruct complex chromosomes like the repeat-rich W sex chromosome and several GC-rich microchromosomes. Telomere-to-telomere assemblies are not a reality yet for most organisms, but by leveraging technology choice it is possible to minimize genome assembly gaps for downstream analysis. We provide a roadmap to tailor sequencing projects around the completeness of both the coding and non-coding parts of the genomes.

Introduction

With the advent of Next Generation Sequencing (NGS) technologies, the field of genomics has grown exponentially and during the last 10 years the genomes of almost 10,000 species of prokaryotes and eukaryotes have been sequenced (from NCBI Assembly database, O'Leary et al. (2015)). Traditional NGS technologies rely on DNA amplification and generation of millions of short reads (few hundreds of bp long) that subsequently have to be assembled into contiguous sequences (contigs; Goodwin et al. (2016)). Although the technique has been revolutionary, the short-read length together with difficulties to sequence regions with extreme base composition poses serious limitations to genome assembly (Chaisson et al. 2015; Peona et al. 2018). Technological biases are therefore impeding the complete reconstruction of genomes and substantial regions are systematically missing from genome assemblies. These missing regions are often referred to as the genomic “dark matter” (Johnson et al.

2005). It is key now for the genomics field to overcome these limitations and investigate this dark matter.

Repetitive elements represent an important and prevalent part of the genomic dark matter of many genomes, given that their abundance and repetitive nature makes it difficult to fully and confidently assemble their sequences. This is particularly problematic when the read length is significantly shorter than the repetitive element, in which case it is impossible to anchor the reads to unique genomic regions. To what extent repeats can hamper genome assemblies depends on whether they are interspersed or arranged in tandem. Highly similar interspersed repeats, like for example transposable elements (TEs), may introduce ambiguity in the assembly process and cause assembly (contig) fragmentation. On the other hand, tandem repeats are repetitive sequences arranged head-to-tail or head-to-head such as microsatellites and some multi-copy genes (e.g., ribosomal DNA and genes of the Major Histocompatibility Complex, MHC). Reads shorter than the tandem repeat array will not resolve the exact number of the repeat unit, resulting in the collapse of the region into fewer copies. Some particular genomic regions enriched for repeats tend to be systematically missing or underrepresented in traditional genome assemblies. These regions include: 1) telomeres at the chromosome ends that are usually composed of microsatellites; 2) centromeres, essential for chromosome segregation often specified by satellites that can be arranged in higher-order structures like the alpha satellite in humans (Willard and Waye 1987) or by transposable elements in flies (Chang et al. 2019); 3) multi-copy genes like MHC genes (Shiina et al. 2009); d) non-recombining and highly heterochromatic chromosomes like the Y and W sex chromosomes (Chalopin et al. 2015; Smeds et al. 2015; Hobza et al. 2017). As these regions play an essential role in the functioning and evolution of genomes, the need to successfully assemble them is a pressing matter.

The other main limitation of traditional NGS methods is the shortcoming in reading regions with extreme base composition (an enrichment of either A+T or G+C nucleotides), thus representing

another source of genomic dark matter. Extreme base composition mainly affects the last step of the standard library preparation for Illumina sequencers that involves PCR amplification (Dohm et al. 2008; Aird et al. 2011). GC-rich regions tend to have higher melting temperatures than the rest of the genome and are thus not as accessible with standard PCR protocols. On the other side of the spectrum, AT-rich regions are also challenging to be amplified with standard PCR conditions and polymerases (Oyola et al. 2012) because they require lower melting and extension temperatures (Su et al. 1996). Several protocols have been developed to help minimize the phenomenon of GC-skewed coverage (uneven representation of GC-rich regions), including PCR-free library preparation (Kozarewa et al. 2009) and isolation of the GC-rich genomic fraction prior to sequencing (Tilak et al. 2018). Nonetheless, there is no single method that entirely solves base composition biases of short-read sequencing and gives a homogeneous representation of the genome (Tilak et al. 2018). As a result, extremely GC-rich or AT-rich regions may not be assembled at all.

It is essential to be aware of technological biases and genome assembly incompleteness during project design since these can affect downstream analysis and mislead biological interpretations (Thomma et al. 2016; Weissensteiner et al. 2017; Domanska et al. 2018; Peona et al. 2018). For example, GC-skewed coverage is particularly important in birds, where 15% of genes are so GC-rich that they are often not represented in Illumina-based genome assemblies (Hron et al. 2015; Botero-Castro et al. 2017). Whether these genes are truly missing or mostly hiding due to technological limitations is still debated (Lovell et al. 2014, Botero-Castro 2017). However the “missing gene paradox” in birds is a clear example of how sequencing technologies can shape our view of genome evolution. Furthermore, some GC-rich sequences can form non-B DNA structures, i.e., alternative DNA conformations to the canonical double helix such as G-quadruplexes (G4). G4 structures are a four-stranded DNA/RNA topologies that seem to be involved into numerous cellular processes, such as regulation of gene expression (Du et al. 2008; Du et al. 2009; Raiber et al. 2011), genetic and epigenetic stability (Schiavone et al. 2014), and telomere maintenance (Biffi et al. 2012). On the repetitive element side,

for example, transposable elements are a major target of epigenetic silencing (Law and Jacobsen 2010) that may influence the epigenetic regulation of nearby genes (Cowley and Oakey 2013; Chuong et al. 2016; Tanaka et al. 2019). The epigenetic effect of transposable elements may be beneficial or deleterious, but in either case it is important to acknowledge their potential involvement in the evolution of gene expression (Lerat et al. 2019). More generally, repetitive elements can play important roles in many molecular and cellular mechanisms, and as a source of genetic variability (Bourque et al. 2018). They have contributed to evolutionary novelty in many organismal groups, by giving rise to important evolutionary features like the mammalian placenta (Emera and Wagner 2012), the vertebrate adaptive immune system (Kapitonov and Koonin 2015; Zhang et al. 2019) and other telomere repair systems (Levis et al. 1993; McGurk et al. 2019). Thus, having genome assemblies that are as complete as possible facilitates research into a multitude of molecular phenomena (Slotkin 2018).

To achieve more complete genomes, we need new technologies. Recently, long-read single-molecule sequencing technologies with virtually no systematic error profile (Eid et al. 2009) have led to more complete and contiguous assemblies (English et al. 2012; Loomis et al. 2013; Pettersson et al. 2019; Smith et al. 2019). To date two sequencing strategies have been developed that produce very long reads from single-molecules: 1) Pacific Biosciences (PacBio) SMRT sequencing, in which the polymerases incorporate fluorescently labelled nucleotides and the luminous signals are captured in real time by a camera; 2) Oxford Nanopore Technologies, which sequences by recording the electrical changes caused by the passage of the different nucleotides through voltage sensitive synthetic pores. These new sequencing techniques have already yielded numerous highly contiguous *de-novo* assemblies (Faino et al. 2015; Gordon et al. 2016; Seo et al. 2016; Bickhart et al. 2017; Weissensteiner et al. 2017; Michael et al. 2018; Yoshimura et al. 2019) and helped improving the completeness of existing ones (Chaisson et al. 2014; Jain et al. 2018), as well as characterizing complex genomic

147 regions like the human Y centromere and MHC gene clusters (Rhoads and Au 2015; Westbrook et
148 al. 2015; Jain et al. 2018; Sedlazeck et al. 2018).
149
150 However, resolving entire chromosomes remains a difficult endeavour even with single-molecule
151 sequencing (except for small fungal and bacterial genomes (Ribeiro et al. 2012; Thomma et al. 2016)).
152 Even though no single technology is able to yield telomere-to-telomere assemblies, it is still possible
153 to bridge separate contigs into scaffolds using long-range physical data and obtain chromosome-level
154 assemblies. Scaffolding technologies are becoming more and more commonly used (Vertebrate
155 Genome Project ; Dudchenko et al. 2017; Belser et al. 2018; Deschamps et al. 2018; Li et al. 2019;
156 Wallberg et al. 2019). The two most common ones are linked-reads (Weisenfeld et al. 2017) and
157 proximity ligation techniques (reviewed in Sedlazeck et al. (2018)). Linked-read libraries are based
158 on a system of labelling reads belonging to a single input DNA molecule with the same barcode
159 (Weisenfeld et al. 2017). In this way, using high molecular weight DNA allows to connect different
160 genomic portions (contigs) that may be distantly located but physically part of the same molecule.
161 High-throughput proximity ligation techniques as Hi-C and CHiCAGO are able to span very distant
162 DNA regions by sequencing the extremities of chromatin loops that could be up to Megabases apart
163 in a linear fashion (for more details see Lieberman-Aiden et al. (2009)). While Hi-C is applied directly
164 on intact nuclei, the CHiCAGO protocol reconstructs chromatin loops *in-vitro* from extracted DNA.
165 All these libraries are then sequenced on an Illumina platform. As linked reads and proximity ligation
166 techniques are becoming more and more popular used nowadays, we also implement and test them
167 in the present study.
168
169 Although a plethora of new sequencing technologies and assembly methods are currently being
170 successfully implemented, it remains unclear how they complement each other in the assembly
171 process. Here we address these assembly and knowledge gaps using a bird as a model. Bird genomes
172 represent a promising target to investigate that as their genomic features make it relatively easy to

assemble most parts with the exception of few complex regions per chromosome. In fact, the typical avian genome is characterized by a small genome size (mean of ~1 Gb Kapusta and Suh (2017); Gregory (2019)) and low overall repeat content (about 10% overall, with the exception of woodpeckers that have 20% (Kapusta and Suh 2017). However, there are gene-rich and GC-rich microchromosomes (Burt 2002; Griffin and Burt 2014; Miller and Taylor 2016) as well as a highly repetitive W chromosomes (at least in non-ratite birds Zhou et al. (2014); Smeds et al. (2015); Bellott et al. (2017)) that are still difficult to assemble.

In this study, to understand which genomic sequences are missing in regular draft genome assemblies with respect to a high-quality and curated assembly, we generated several draft *de-novo* genomes and a reference genome for the same sample of the paradise crow (*Lycocorax pyrrhopterus*, 'lycPyr'). The paradise crow is a member of the birds-of-paradise family (Paradisaeidae), one of the most prominent examples of an extreme phenotypic radiation driven by strong sexual selection, and as such, a valuable system for the study of speciation, hybridization, phenotypic evolution and sexual selection (Shedlock et al. 2004; Irestedt et al. 2009; Ligon et al. 2018; Prost et al. 2019; Xu et al. 2019). We sequenced one female paradise crow individual with all the technologies that worked with a DNA sample of mean 50 kb molecule length. We combined short, linked, and long-read libraries together with Hi-C and CHiCAGO proximity ligation maps into a multiplatform reference assembly. All these technologies permitted us to curate the resulting assembly by controlling for consistency between multiple independent data types and make majority rule decision in conflicting cases. The curated assembly enabled us to: 1) demonstrate the feasibility of obtaining a high-quality assembly of a non-model organism with limited sample amount and non-optimal sample quality (a situation that empiricists commonly face); 2) identify which genomic regions are actually gained from combining technologies compared to draft assemblies of each individual technology; 3) assess the strengths and weaknesses of the implemented technologies regarding the efficiency of assembling difficult repeats and GC-rich regions; and 4) quantify how technologies can widen or limit the study

of specific genomic features (e.g., TEs, satellite repeats, MHC genes, non-B DNA structures), thus providing a roadmap to investigate them.

Results

We leveraged the power of data generated from multiple sequencing approaches for the same sample of paradise crow to generate a gold-quality assembly and to assess limitations of regular draft genomes based on any single technology. Briefly, we combined short, linked and long reads with proximity-ligation data to obtain a high-quality assembly despite the limitations of a non-model organism such as limited sample amount and non-optimal quality. For each sequencing technology, we produced an independent *de-novo* assembly. These assemblies were compared using majority-rule decisions by manually curating the final assembly. Finally, the multiplatform assembly was compared to each *de-novo* version to assess the amount of repeats and other complex regions previously missing from the individual assemblies. We then evaluated the completeness of each assembly using a variety of different metrics, including established scores such as BUSCO, contig/scaffold N50, LTR Assembly Index and new metrics like overall repeat content, number of MHC IIB exons, GC and G4 content, as well as number and nature of gaps.

Long and short read *de-novo* assemblies

In order to compare the efficiency of short, linked, and long reads, we produced independent draft assemblies for each of the different sequence libraries. One draft genome assembly of *L. pyrrhopterus* based on short reads (Illumina) is already available from Prost et al. (2019) ('lycPyrIL'; **Table 1**). For the present study, we produced two linked-read libraries (10X Genomics Chromium) from which we assembled two draft genomes ('lycPyrSN1' and lycPyrSN2'; where 'SN' stands for Supernova) and a PacBio library from the same paradise crow sample that generated the primary assembly

'lycPyrPB' (**Table 1** and **Methods** section). In total, four independent *de-novo* assemblies were generated.

We first evaluated the completeness of these assemblies by assessing their fragmentation, contig and scaffold N50 and by counting the number of core genes present with BUSCO (Nishimura et al. 2017; Waterhouse et al. 2017). In terms of fragmentation, the PacBio primary assembly ('lycPyrPB') consisted of about 3,000 contigs, while lycPyrIL had ~3,000 scaffolds, and the 10XGenomics assemblies had about ~14,000 scaffolds (**Table 1**). The short and linked-read assemblies all had a scaffold N50 of about 4 Mb while the PacBio assembly had a contig N50 of 6 Mb (**Table 1, Supplementary Table S1**). Notably, there is a 10-times higher of contig N50 in lycPyrPB relative to the lycPyrIL assembly, indicating significant improvement in assembly continuity in the PacBio vs. Illumina assembly. Next, we used the BUSCO tool (Nishimura et al. 2017) to identify correctly assembled core genes (percentage of only single-copy and complete genes follow): lycPyrIL 93.8%, lycPyrSN1 92.5%, lycPyrSN2 91.5%, lycPyrPB 84.8% prior to any assembly polishing (**Supplementary Table S2**). Similarly, we estimated genome completeness and quality of the intergenic and repetitive sequences with the LTR Assembly Index (LAI, Ou et al. (2018)). This index is calculated as the proportion of full-length LTR retrotransposons over the total length of full-length LTR retrotransposons plus their fragments. LAI could only be calculated for lycPyrPB since the other *de-novo* assemblies did not have enough complete LTR elements for the algorithm to work. lycPyrPB has an LAI score of 11.89, which is typical of a reference-quality assembly (Ou et al. 2018), and higher than chicken (galGal5, RefSeq accession number GCF_000002315.6; Bellott et al. (2017)) with an LAI score of 7.54. We cannot exclude that the higher score in paradise crow is caused by biological differences in LTR load between the species. More details about the LAI score distribution across chromosomes and genomes are found in **Supplementary Table S3, Supplementary Figure S1** and **Supplementary Figure S2**.

Table 1. Draft and multiplatform assemblies generated for the paradise crow. For each assembly the sequencing technology and software used to produce them are shown together with contig N50, scaffold N50 and the number of gaps.

Assembly	Technology	Software	Contig N50 (bp)	N contigs	Scaffold N50 (bp)	N scaffolds	N gaps[a]	Missing assembly[b] (%)
lycPyrIL	Illumina HiSeq2500 (PE + MP)[c]	ALLPATHS-LG	620,719	10,766	4,227,710	3,216	14,573	3.82
lycPyrPB	PacBio RSII C6-P4	Falcon	6,644,420	3,422	-	-	-	0.45
lycPyrSN1	10X Genomics Chromium HiSeqX	Supernova2	144,856	29,791	4,360,585	13,934	21,550	4.53
lycPyrSN2	10X Genomics Chromium HiSeqX	Supernova2	149,640	27,366	4,748,626	14,217	20,131	2.62
lycPyrHiC	PacBio + Phase Genomics Hi-C	Proximo	6,644,420	3,422	70,588,898	2,927	533	0.45
lycPyrILPB	lycPyrIL + gap-filling with PacBio	PBJelly	1,982,606	6,895	4,229,628	3,216	10,422	3.03
lycPyr2	PacBio + Dovetail CHiCAGO	HiRise	6,294,665	3,463	6,644,037	3,227	282	0.45
lycPyr3	lycPyr2 + 10X Genomics	ARCS + LINKS	6,294,665	3,463	8,009,555	3,121	345	0.27
lycPyr4	lycPyr3 + Phase Genomics Hi-C	Proximo	6,294,665	3,463	69,071,023	1,713	1,791	0.27
lycPyr5	lycPyr4 + manual curation with alignments + gap filling	PBJelly	7,540,011	3,269	74,173,823	1,700	1,631	0.001
lycPyr6	lycPyr5 + manual curation with Hi-C	Juicer	7,540,011	3,271	74,173,823	1,700	1,635	-

[a] The number of gaps is estimated as the count of stretches of N nucleotides within a scaffold.
[b] The percentage of incompleteness is relative to the final version of the multiplatform assembly: (1 – (assembly size / final assembly size)) * 100. The N nucleotides are excluded from the calculation.
[c] PE: paired end reads; MR: mated reads.

The multiplatform reference assembly

To generate a high-quality genome assembly, we combined five technologies (short, linked, and long reads in addition to a CHiCAGO and Hi-C proximity ligation maps) into one multiplatform assembly. This process was divided into 9 steps (**Figure 1**), described in further detail in the **Methods** section.

First, we assembled the PacBio long reads into the primary assembly (lycPyrPB; 3,442 contigs) and it was scaffolded and corrected for misassemblies with the Dovetail CHiCAGO map ('lycPyr2'; **Figure 1a-b**). The scaffolding software HiRise introduced 98 breaks and made 293 joins of scaffolds (gaps of 100 bp were introduced at this stage), as well as closed 11 gaps between contigs and resulted into an assembly of 3,227 scaffolds (**Table 1** and **Supplementary Table S1**). Subsequently we polished the assembly with long reads (two rounds of Arrow; Chin et al. (2016)) and short reads (two rounds of Pilon; Walker et al. (2014); **Figure 1c**).

We then continued to scaffold lycPyr2 with two types of long-range information in order to get a chromosome-level assembly. First, we used 10X Genomics linked reads (SN1 library; 24 kb mean molecule length; **Figure 1d**) that encode medium-range spatial information that placed 235 contigs into 131 new scaffolds. Of these new scaffolds we kept only 88 and discarded potential chimeric scaffolds, which were identified by being composed of sex-linked contigs and autosomal ones (based on male/female short-read coverage; see **Methods**). We then confirmed the chimeric nature of such scaffolds by constructing an additional assembly based on scaffolding lycPyrPB with the Hi-C map ('lycPyrHiC'; **Table 1**). Phase Genomics Hi-C, i.e., 3D chromatin conformation data, can bridge sequences megabases apart (Burton et al. 2013) and theoretically reconstruct entire chromosomes (Hi-C super-scaffolds). In this way lycPyrHiC represented a second independent verification of the collinearity or chimeric nature of the contigs. Accordingly, we checked whether the contigs resided on different Hi-C super-scaffolds. Once we removed the chimeric contigs, we obtained 'lycPyr3' that contained a total of 3,121 scaffolds. Secondly, we scaffolded lycPyr3 with Phase Genomics Hi-C and

obtained 38 super-scaffolds ('lycPyr4'; **Figure 4e**) that harboured 1,446 contigs/scaffolds and accounted for 97% of the assembly, while 1,675 contigs/scaffolds remained unplaced (3%). As most of these super-scaffolds (32 out of 38) correspond to entire chromosomes of other avian species, we call them "chromosome models". Examining the post-scaffolding Hi-C heatmap, we found that chromosomes 1 and 2 were split into two Hi-C super-scaffolds, respectively. Therefore, following the high level of Hi-C interaction between these super-scaffold pairs in the heatmap (**Supplementary Figure S3**), we manually combined the respective super-scaffold pair into one chromosome model (see **Methods**); the assembly thus resulted in 36 chromosome models.

We proceeded to further manually curate the chromosome models by looking for misassemblies (**Figure 1f**) and used long reads for gap-filling (**Figure 1g**). We corrected fine scale orientation issues of contigs within scaffolds through whole genome alignments (see **Figure 2** and **Methods**) and corrected more orientation, order issues and erroneous chromosomal translocations through the inspection of Hi-C heatmaps (see **Figure 1i** and **Methods**). We first corrected 43 misassemblies by aligning the draft genomes and three outgroups to lycPyr4 (**Figure 2** and **Methods**). Next, we extended contig ends and filled scaffold gaps with long reads using PBJelly ('lycPyr5'). PBJelly filled 106 gaps, extended 56 gaps on both ends and extended only one end of 292 gaps (**Supplementary Table S4**). Finally, we further checked for misassemblies with the help of the Hi-C data. We generated a Hi-C heatmap of lycPyr5 with Juicer (Durand et al. 2016) and detected misassemblies though the visual inspection of such a map with JuiceBox (Dudchenko et al. 2018) following the indications given by (Lajoie et al. 2015) and (Dudchenko et al. 2018). The Hi-C heatmap showed mostly orientation and ordering problems within lycPyr5 (**Supplementary Figure S4**) that can be identified from the ribbon-like patterns in the interaction map (Dudchenko et al. 2018). Finally, the map highlighted the misplacement of two contigs between chromosome models (**Supplementary Figure S4**). In total 76 misassemblies were corrected to generate the final assembly ('lycPyr6') with a scaffold N50 of ~75 Mb (**Table 1**).

In parallel to the assembly of lycPyr6, we also generated a simpler multiplatform assembly by gap-filling the Illumina primary assembly (lycPyrIL) with PacBio reads ('lycPyrILPB'). PBJelly was used to gap-fill the Illumina assembly and successfully closed 4,151 gaps, reducing the total number of gaps from 14,573 to 10,422. It also double extended 418 gaps and single extended 2,597 gaps (**Supplementary Table S4**). The numbers of scaffolds and scaffold N50 did not significantly change from lycPyrIL (**Table 1**).

Chromosome models: macrochromosomes, microchromosomes and sex chromosomes

We obtained 36 chromosome models comprised of 16 macrochromosome models, 18 microchromosome models and two sex chromosome models. All the macrochromosome models showed homology to chicken chromosomes and were named after their homologous counterparts. The same applies for 12 of 18 microchromosomes, while the remaining 6 showed no homology with chicken chromosomes and therefore were tentatively named as unknown chromosomes "chrUN1-6". The chromosomes homologous to chicken are mostly syntenic with respect to chicken with few exceptions. In fact, chicken chromosome 1 and 4 are split in two in Passeriformes and correspond, respectively, to chromosome 1 and 1A, and chromosome 4 and 4A (Kapusta and Suh 2017).

The Z and W sex chromosome models had an assembled size of 73.5 Mb and 21.4 Mb, respectively, and were comparable to chicken (82 Mb and 7 Mb, galGal6a, RefSeq accession number GCF_000002315.6; Bellott et al. (2017)). Z and W models were also largely consistent with the sex-linked contigs previously identified using male/female coverage comparisons (**Supplementary Table S5** and **Methods**), only 3.11 Mb of the W and 3.99 Mb of the Z chromosome were contigs not previously identified as sex-linked. Finally, the pseudoautosomal region (PAR) seemed to be fragmented into two parts. We identified two contigs that are homologous to the PAR of flycatcher; one of them was placed by Hi-C onto the Z while the other was placed onto the W chromosome model (**Supplementary Table S5**). While the Z chromosome showed a repetitive content similar to the

autosomes (~10%), the W was extremely repeat-rich (~70%, **Figure 3a, Supplementary Table S6**). The dotplots of the alignments of the paradise crow sex chromosomes with the chicken sex chromosomes (**Supplementary Figure S5 and Supplementary Figure S6**) showed that the two Z chromosomes had a high level of synteny and collinearity while the repetitiveness of the two W chromosomes made it difficult to identify shared single-copy regions other than very small ones. The sex chromosomes were also easily identified in the post-clustering Hi-C heatmap (**Supplementary Figure S3**), as their hemizygosity can be expected to result in roughly half of the amount of Hi-C interactions (calculated as the frequency of shared paired-end reads between contigs/scaffolds) within each chromosome model and with the other chromosome models.

Finally, the LTR Assembly Index calculated on the single chromosomes yielded high scores (min 0 on chromosome 10, mean 13.14, max 21.41 on chromosome W) that have been suggested to be indicative of reference and gold-quality assemblies (Ou et al. (2018), **Supplementary Figure S1** and **Supplementary Table S3**).

GC content and G4 motif prediction

GC-rich regions are commonly underrepresented in traditional NGS assemblies because of the aforementioned GC-skewed coverage phenomenon (see **Introduction**). Comparing the different *de-novo* assemblies, we noticed that indeed lycPyrPB showed more GC-rich regions (54,532 windows of 1 kb size with GC > 58.8%) with respect to lycPyrIL, SN1 and SN2 (45,966, 45,720 and 52,080 such windows, **Figure 3b**, **Supplementary Table S7**, **Supplementary Figure S7**). Thus, lycPyrSN1 shared a similar number of GC-rich regions while lycPyrSN2 was closer to lycPyrPB (**Supplementary Figure S7**, **Supplementary Table S7**).

Since GC-rich regions may form G-quadruplexes motifs and structures (G4), we expected the depletion of GC-rich short reads to limit the representation of G4 motifs in short read assemblies. Conversely, we expected G4 motifs to be more abundant in long read assemblies, since these have

been suggested to be virtually free from sequence-based biases (Eid et al. 2009). To test this, we predicted the presence of G4 motifs using Quadron (Sahakyan et al. 2017) in all the different assemblies. All the *de-novo* Illumina-based assemblies had fewer predicted G4 sites the PacBio assemblies (**Figure 3c** and **Supplementary Table S8**). lycPyrSN2 and lycPyrIL had 7.3 and 7.5 Mb (169,214 and 166,602 motifs) occupied by G4 sequences and about 1.6 Mb or 24,000 motifs less than lycPyr6 (9.1 Mb, 193,248 motifs). lycPyrSN1 was the assembly with the fewest G4 motifs predicted (6.5 Mb, 149,275 motifs). The PacBio primary assembly lycPyrPB had 8.42 Mb of predicted G4, which was slightly higher in lycPyr2 after the correction with Dovetail CHiCAGO (8.43 Mb; **Figure 3c** and **Supplementary Table S8**). In the final assembly lycPyr6, G4 motifs were more present on microchromosomes than on macrochromosomes (**Figure 3d**).

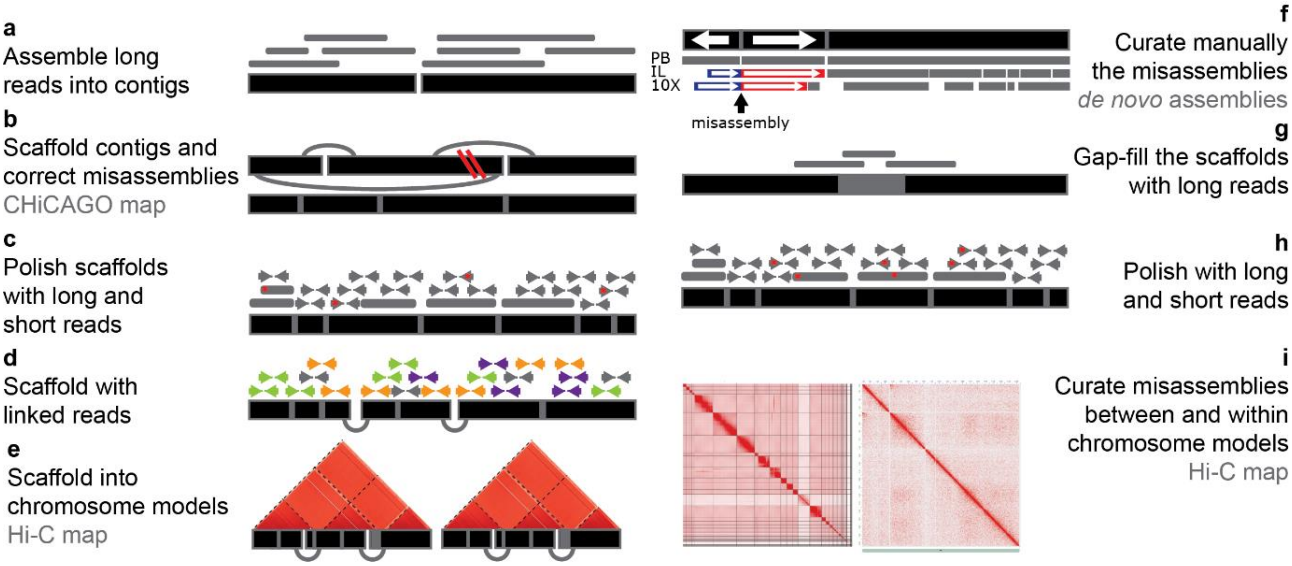

Figure 1. Overview of the multiplatform assembly process. **(a)** Long reads were assembled into contigs. (**b)** The primary assembly was corrected and scaffolded using long-range information provided by the CHiCAGO proximity ligation map. **(c)** The assembly was then polished from base-calling errors with both short and long reads and **(d)** further scaffolded with linked-reads. **(e)** The scaffolds are ordered and oriented into chromosome models according to the Hi-C proximity ligation map. **(f)** The chromosome models were aligned to the *de-novo* assemblies based only on one single technology and then manually inspected to find misassemblies and correct them following the majority rule (more details in **Figure 2** and **Methods**). PB: PacBio long-read assembly; IL: Illumina short-read assembly; 10X: 10XGenomics linked-read assemblies **(g)** Long reads were used to gap-fill the assembly and **(h)** to polish the final version together with short reads. **(i)** Hi-C heatmaps were used to identify and correct misassemblies between and within chromosome models.

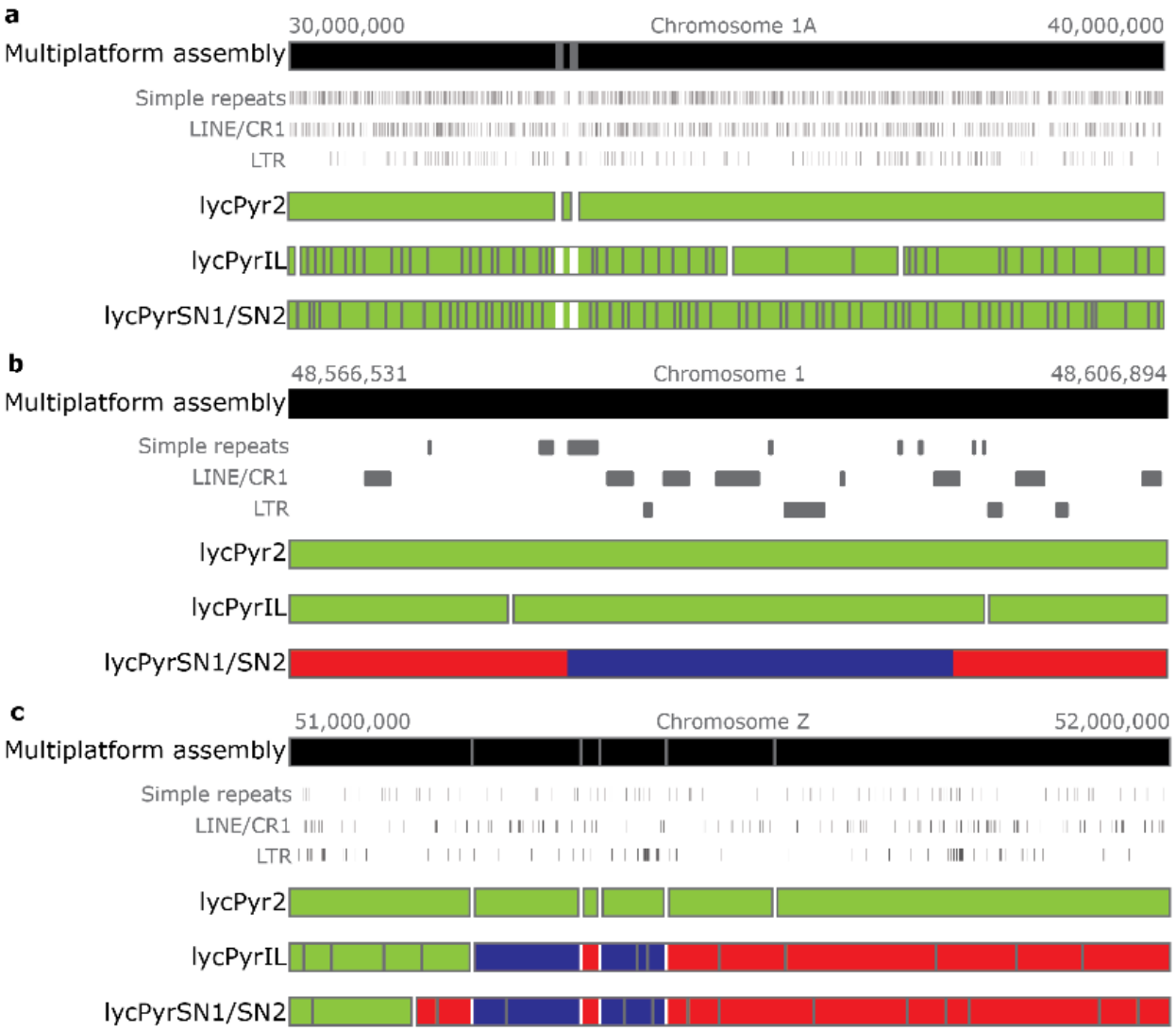

Figure 2. Examples of the manual curation of the assembly (**step f** in **Figure 1**). The multiplatform assembly is aligned to the other *de-novo* assemblies from the same sample. The grey lines within the assemblies represent gaps between different contigs or scaffolds while the white lines represent gaps within the same scaffold. Green means that the contigs/scaffolds align to the reference in the same orientation for their entire length while red and blue highlight contigs/scaffolds that partially align in the forward (red) and reverse (blue) direction to the reference. **(a)** Here 10 Mb of chromosome 1A are shown that are in accordance with all the *de-novo* assemblies. Nonetheless, short-read based technologies yielded much more fragmented scaffolds. **(b)** Example of a scaffold orientation misassembly in the 10XGenomics assembly. The other two assemblies span the inverted region and both agree with the multiplatform assembly. **(c)** Example of how two different assemblies could help to identify which contigs have to be re-oriented and re-ordered in the final assembly. In lycPyrIL, lycPyrSN1 and lycPyrSN2 we had scaffolds than span the misoriented (blue) region and bridge it to contigs that showed concordant orientation with the multiplatform assembly. This indicated that we have only a small local inversion of two PacBio contigs

Repeat library

To obtain an in-depth annotation of interspersed and tandem repeats, the *de-novo* characterization of repetitive elements and manual curation thereof are essential (Platt et al. 2016). We manually curated a total of 183 consensus repeat sequences generated from lycPyrIL and lycPyrPB to have an optimal repeat characterisation. In Prost et al. (2019) a total of 112 raw consensus sequences were produced using RepeatModeler on three Illumina-based birds-of-paradise (*Astrapia rothschildii*, *L. pyrrhopterus* and *Ptiloris paradiseus*; including lycPyrIL) but only the 37 most abundant from lycPyrIL were manually curated. We then curated the remaining 75 and added 71 more *de-novo* consensus sequences based on curated raw consensus sequences from RepeatModeler run on lycPyrPB. Our new bird-of-paradise specific repeat library is now composed of the following numbers of consensus sequences: 56 ERVK, 56 ERVL, 37 ERV1, 5 CR1, 4 LTR, 9 satellites, 2 DNA transposons, 1 SINE/MIR, and 13 unknown repeats. All the consensus sequences curated for the three species of birds-of-paradise (*L. pyrrhopterus*, *A. rothschildii*, *P. paradiseus*) are given in **Supplementary Table S9**. Eventually, we merged birds-of-paradise consensus sequences together with the Repbase Aves library, the flycatcher (Suh et al. 2018), the blue-capped cordon blue (Boman et al. 2019) and the hooded crow libraries (Weissensteiner et al. 2019).

Custom and *de-novo* repeat libraries substantially improve the identification and masking of repeats in genome assemblies (Platt et al. 2016). To quantify this effect for our assemblies, we compared a general avian repeat library with our curated one. The custom library resulted in masking a higher fraction of the genome in every assembly (**Figure 3e-f**). When comparing the masked fraction with the custom library to the fraction masked with the Repbase library, we see that lycPyrIL, lycPyrILPB, and lycPyrSN1 have 20% more masked repeats (from 78 Mb to 94 Mb), while lycPyrSN2 has 21.68% (from 83 to 101 Mb), lycPyrPB 38% (from 87 Mb to 120 Mb), and lycPyr6 38% (from 88 Mb to 122 Mb; see **Figure 3e**, **Supplementary Table S10**). In particular, with the new library we were able to identify 9.4 Mb of satellite DNA in the PacBio-based assemblies, while the standard Repbase avian library identified only 1 Mb (**Figure 3e-f**, **Supplementary Table S10**). Relative to lycPyr6, most of

420 the satellites and unknown repeats remain unassembled in the short-read and linked-read assemblies

421 (**Figure 3f** and **Figure4b**).

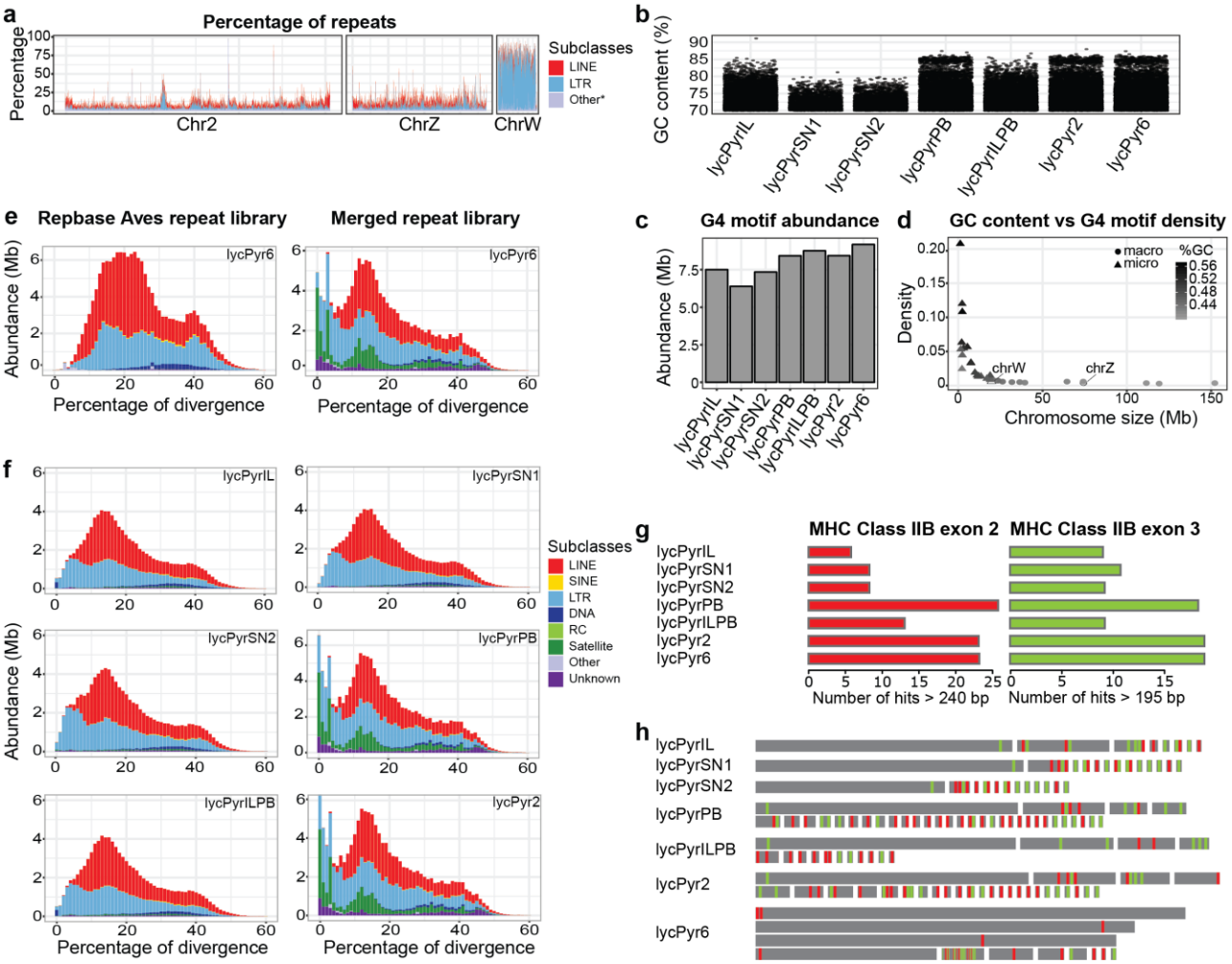

422

423

424 **Figure 3**. **(a)** Comparison of the repeat content across chromosome 2 (representative of autosomes),
425 Z and W calculated as the percentage of repeats per window of 50 kb. Here LINE and LTR are
426 shown as major components of the mobile element repertoire and all the other types of repeats are
427 merged into the "Other*" category. **(b)** Distribution of GC-content per window (10 kb) across
428 assemblies on the left side of the violin plots. GC-content distribution of the windows containing
429 G4 motifs on the right side of the violin plots. **(c)** G4 motif abundance across different paradise
430 crow assemblies. (**d**) G4 motif density across the chromosome models of the final assembly; the
431 chromosomes are arranged by size; macrochromosomes are coloured in light grey while
432 microchromosomes (smaller than 20 Mb) are shown in dark grey. The density distribution of G4 in
433 micro and macro chromosomes was statistically different (t-test p-value: 0.01). **(e)** Repeat landscape
434 of lycPyr6 masked with the Repbase Aves repeat library (on the left) and masked with the custom
435 library produced in this study which also included the Repbase Aves library (on the right). **(f)**
436 Repeat landscapes of the four *de-novo* assemblies of the paradise crow masked with the custom
437 repeat library. **(g)** Abundance of MHC class IIB exon 2 and exon3 in the different paradise crow
438 assemblies. **(h)** Schematic visualization of the instances of MHC class IIB exon 2 (red) and 3
439 (green). Each black rectangle represents a different contig or scaffold.

440

441 **MHC class IIB analysis**

442 In birds, the multi-copy gene family of the major histocompatibility complex (MHC) is arranged as
443 a megabase long tandem repeat array (Miller and Taylor 2016). Since we expect it to be even more
444 difficult to correctly assemble than the aforementioned interspersed repeats (O'Connor et al. 2019),
445 it represents a prime candidate region for measuring the quality of an assembly.

446

447 We used the presence of entire copies of the second (most variable) and third (more conserved) exons
448 of the MHC class IIB as proxies of assembly quality (Hughes and Yeager 1998). Overall, we found
449 that short-read assemblies had fewer MHC gene copies than long-read assemblies (**Figure 3g-h**),
450 while linked-read assemblies performed better than Illumina alone. Regarding exon 2 (**Figure 3g**),
451 PacBio retrieved 26 copies while Illumina and 10XGenomics assembly only hold 6-8. However, it is
452 worth noting that after correcting lycPyrPB with the Dovetail CHiCAGO map, 3 copies were lost
453 (not detectable as full-length exons anymore) and were not restored by the subsequent steps of
454 sequence corrections and curation. The results were similar for exon 3 (**Figure 3g**): PacBio
455 assemblies retrieved 18-19 copies while the other technologies retrieved only 9-11 copies. In this case
456 we see that the molecule input length of 10XGenomics library has an effect on the assembly of these
457 genes, where the library with shorter molecule length had assembled more copies than the longer one
458 (11 vs 9 exon 2 copies; **Figure3g-h**). On the other hand, while Dovetail CHiCAGO prevented the
459 identification of some exon 2 copies, it increased the number of assembled copies of exon 3.

460

461 **Gap analysis**

462 The process of scaffolding links contigs together without adding any information about the missing
463 DNA between them, but it is possible to use long reads to fill those gaps. For this we utilized PBJelly
464 (English et al. 2012) to extend and bridge contigs in the assembly by locally assembling PacBio reads
465 to the contig extremities. Once the software finds reads aligned to the contig extremities, the
466 extremities can be: 1) extended on one or both sides to reduce the gap length, 2) extended and bridged

467 to fill the entire gap, 3) extended over the length of the gap without being ultimately bridged
468 (overfilled). PBJelly extended the extremities of 348 gaps, closed 116 gaps and overfilled 236 gaps
469 (**Supplementary Table S4**). This gap-filling step added a total of 2.96 Mb to the assembly. All the
470 sequences that were extended or gap-filled were more GC-rich (40%-89%, mean 58%) than the
471 average GC content of 40% and 2865 G4 motifs were added for a total of 171 kb. Only 800 kb of the
472 2.96 Mb added were repetitive elements; specifically, ~400 kb of LTR elements were added, 120 kb
473 of LINE, 142 kb of satellite DNA and 90 kb of simple and low complexity repeats (**Supplementary**
474 **Table S4**).
475
476 Furthermore, we investigated the causes of assembly fragmentation in several assemblies by
477 analysing the immediate adjacency of repetitive elements to the gaps (lower part of **Figure 4a**). We
478 found that simple repeats were the major fragmentation cause in Illumina and 10XGenomics
479 assemblies, followed by LTR and LINE elements (**Figure 4c-d**). In contrast, PacBio gaps (lycPyrPB
480 and lycPyr2) seemed to be mainly caused by LTR elements and secondarily by satellites (**Figure 4c-**
481 **d**).
482

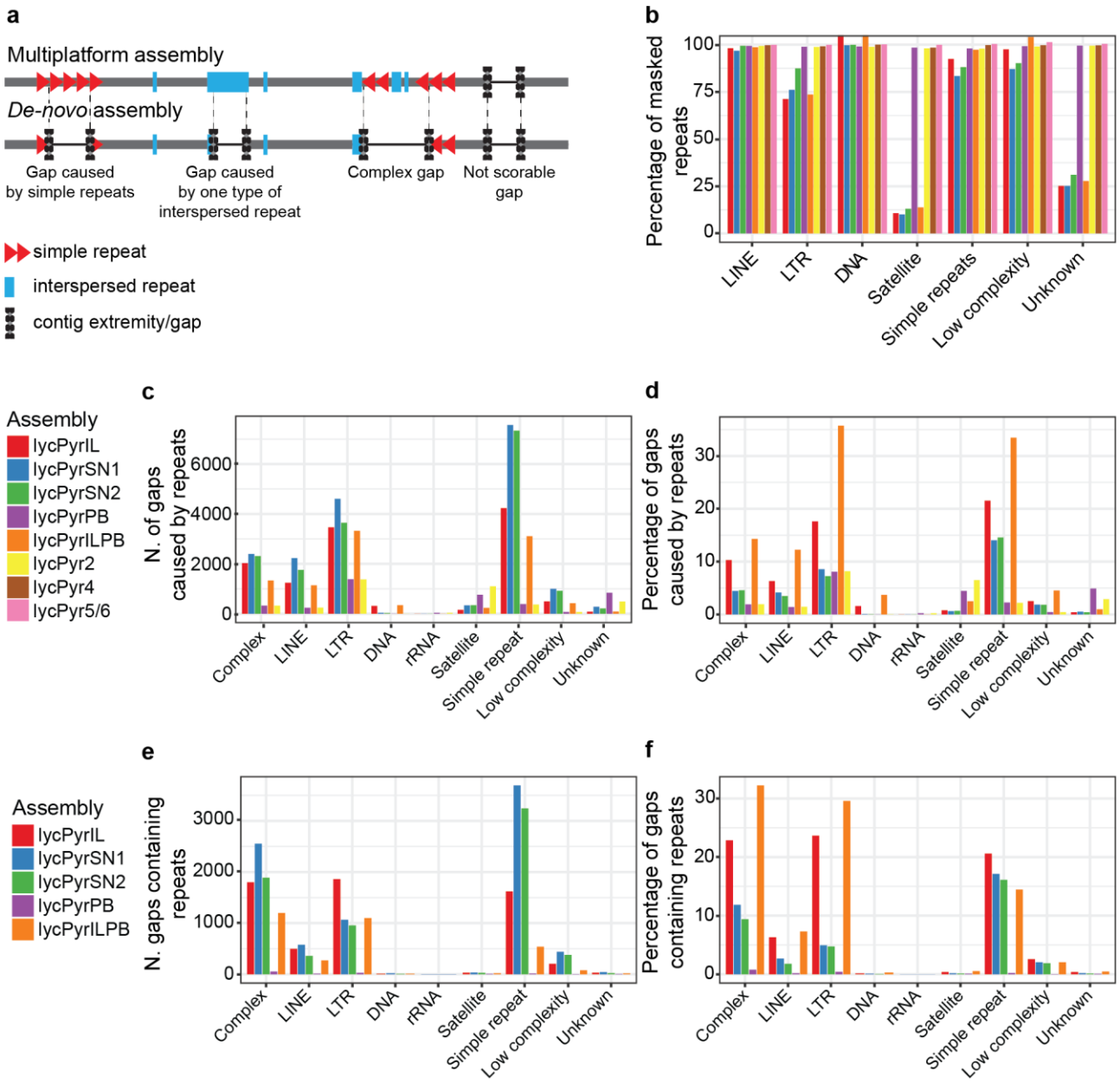

Figure 4 Overview of the causes and content of gaps in the paradise crow assemblies by comparing all the assembly versions to the final version. **(a)** Schematic representation of how gaps were categorized based on the flanking regions and content. **(b)** Proportion of repeats present in each assembly version respect to the reference (lycPyr6). **(c)** Number of gaps caused by the major repeat groups. **(d)** Proportion of gaps caused by the major repeat groups. (**e**) Number of gaps that contain (map to) repeats. (**f**) Proportion of gaps that contain (map to) repeats.

Finally, we quantitatively and qualitatively assessed which repeats in the final multiplatform assembly lycPyr6 were collapsed as gaps in the draft assemblies (**Figure 4e-f**). Many gaps in the Illumina and 10XGenomics draft assemblies corresponded to complex regions consisting of multiple types of repetitive elements (**Figure 4e-f**). Among draft assembly gaps containing only a single type

of repeat in lycPyr6, most were caused by simple repeats, LTR retrotransposons, and LINE retrotransposons in short-read and linked-read assemblies (**Figure 4e-f**).

Discussion

Assembling complete eukaryotic genomes is a complex and demanding endeavour often limited by technological biases and assembly algorithms (Alkan et al. 2010; Sedlazeck et al. 2018). In the last decade, NGS technologies defined the standard of genome assemblies. Although they provided an unprecedented view on the structure and evolution of many coding regions (Zhang et al. 2014), short reads hardly inform on the entire complexity of a genome (Thomma et al. 2016). Indeed, the systematic absence from genome assemblies and the difficulty to characterize the nature of many such genomic regions (e.g. centromeres, telomeres, other repeats and highly heterochromatic regions) gave these "unassemblable" sequences the evocative name of genomic "dark matter" (Johnson et al. 2005; Weissensteiner and Suh 2019).

In this study, we demonstrated that a combined effort involving multiple state-of-the-art methods for long-read sequencing and scaffolding yielded a high-quality reference for a non-model organism. We showed that a multiplatform approach was highly successful in resolving elevated quantities of genomic dark matter in respect to single-technology assemblies (regular draft assemblies) and thus resulted in a much more complete assembly. In order to assess genome completeness we focused mostly on the quantification and characterization of previously inaccessible regions within genomic dark matter, such as large transposable elements, GC-rich regions, and the high-copy MHC locus.

We generated a *de-novo* multiplatform assembly of a female bird-of-paradise genome by combining the cutting-edge technologies that are now being implemented in many assembly projects (Faino et al. 2015; Gordon et al. 2016; Seo et al. 2016; Bickhart et al. 2017; Weissensteiner et al. 2017; Michael

et al. 2018; Yoshimura et al. 2019), namely Illumina short reads, 10XGenomics linked reads, PacBio long reads and two proximity ligation maps with Dovetail CHiCAGO and Phase Genomics Hi-C. The choice of using a bird-of-paradise is manifold. First, avian genomes are small among amniotes and have an overall repeat content of 10%, which make most genomic regions relatively "easy" to assemble. This has made it possible to focus on regions that are challenging to assemble in eukaryotic genomes of any size and complexity, like the repeat-rich W sex chromosome, and the GC-rich microchromosomes. Second, birds-of-paradise is a highly promising system for the study of speciation, hybridization and sexual selection (Irestedt et al. 2009; Prost et al. 2019; Xu et al. 2019). A gold standard genome for this family will consequently expose new possibilities for more in-depth studies of the genomic evolution behind the spectacular radiation of birds-of-paradise.

By employing a multiplatform approach, we 1) could assemble a chromosome-level genome which includes the W chromosome and several previously inaccessible microchromosomes (i.e., comparable to the chicken genome, so far the best avian genome available); 2) report that a substantial proportion (up to 90%) of repeat categories like satellites and LTR retrotransposons are missing from most types of *de-novo* assemblies (**Figure 3e-f**, **Figure 4b**); and 3) identify simple repeats and LTR retrotransposons as the major causes of assembly fragmentation (**Figure 4c-d**).

A chromosome-level assembly for a non-model organism

Our final assembly comprises 36 chromosome models. This assembled chromosome number is similar to the known karyotype of another bird-of-paradise species *Ptiloris intercedens* (36-38 chromosome pairs; Les Christidis, personal communication). Among these models, there are 16 macrochromosomes, 12 microchromosomes, and the Z and W sex chromosomes showing homology to chicken chromosomes (galGal6a). The remaining 6 models do not share homology with known chicken chromosomes (galGal6a) and they might be putatively uncharacterized microchromosomes. Microchromosomes are known to be very GC-rich (Burt 2002) and indeed this trend is present in our

data as well (**Figure 3d**). Base composition can create biases during the sequencing process especially when a PCR step is required for the library preparation (Dohm et al. 2008; Aird et al. 2011) thus limiting the representation of GC-rich and AT-rich reads in the data. Although, long read sequencing technologies like PacBio have reduced amplification-based biases to a minimum (Schadt et al. (2010) but see Guiblet et al. (2018)), we could not assemble contiguous sequences for all microchromosomes. Among the unknowns and unassembled chromosomes, chromosome 16 which is one of the most complex avian chromosomes and also holds the MHC (Miller and Taylor 2016). The absence of these chromosomes is likely explained by that they are by far the densest in G4 motifs of all chromosomes (**Figure 3d**). Given that DNA polymerase tends to introduce sequencing errors in the presence of G4 structures (Guiblet et al. 2018), it is tempting to think that the depletion of microchromosomes from assemblies is not only due to GC content per se but also due to the potential presence of non-B structures (like G4) that elevated GC content appears to correlate with. Nonetheless, even with the extensive use of cytogenetics the last chicken assembly (galGal5; Warren et al. (2017)) completely lacks 5 microchromosomes. It thus seems plausible that these chromosomes need special efforts to be recovered.

One of the most surprising outcomes of this multiplatform approach is the successful assembly of the highly repetitive W chromosome which turned out to be larger (assembly size 21 Mb) and more repetitive than the chicken equivalent (assembly size 9 Mb; Bellott et al. (2017)). In both species, it is likely that the assembled sequences cover the euchromatic portions of the W. Birds have a ZW sex chromosome system where the female is the heterogametic sex and the female-specific W is analogous to the mammalian male-specific Y chromosome. Comparable to the mammalian Y (Charlesworth et al. 2000), the W chromosome is highly repetitive and difficult to assemble (Weissensteiner and Suh 2019). Previous studies focusing on the repetitive content of the avian W in chicken (Bellott et al. 2017) and collared flycatcher (Smeds et al. 2015) showed in both cases a repeat density of about 50%. In our assembly of the paradise crow, we found the W chromosome to be even

more repetitive with a repeat density of ~70% and highly enriched for LTR retrotransposons (**Figure 3a** and **Supplementary Table S6**). Having assembled chromosomes is key to improve any genomic analysis but studies on sex chromosome evolution in birds has so far been heavily biased towards Z (Zhou et al. 2014; Yazdi and Ellegren 2018; Xu et al. 2019). With genome assemblies like the present, it will be possible to improve reconstructions how the two sex chromosomes diverged. We can already see that the W chromosome evolves rapidly (**Supplementary Figure S5**) via accumulation of transposable elements and only few regions appear syntenic between paradise crow and chicken W.

How complete are genome assemblies?

Previous studies (see for example Etherington et al. (2019); Paajanen et al. (2019)) have assessed the efficiency of available sequencing technologies in genome assembly and genome completeness mainly through summary statistics like scaffold N50 and BUSCO. Scaffold N50 indicates the minimum scaffold size among the largest scaffolds making up half of the assembly, while BUSCO values measure the number of complete/incomplete/missing core genes in the assembly. However, genome completeness goes beyond scaffold N50 and gene presence (Thomma et al. 2016; Domanska et al. 2018; Sedlazeck et al. 2018). Genes usually occupy a small fraction of genomes and new sequencing technologies commonly yield high N50 values. Therefore, these statistics have a very limited scope in perspective of what the new sequencing technologies can achieve.

Although often being used as proxy of assembly quality, scaffold N50 is hardly meaningful in this regard since it does not inform about the completeness and correctness of the assembled sequences. If we order the scaffolds by decreasing size, scaffold N50 value can only reflect the fragmentation level of the first half of the assembly regardless of whether the second half is made up of shorter sequences. Finally, contig N50 should be used as a measure of contiguity, rather than scaffold N50, as contig length measures sequences not interrupted by gaps.

Most of the currently available avian genomes score more than 94% of BUSCO gene completeness (Peñalba et al. 2019) with various degrees of fragmentation, suggesting that it has become straightforward to generate short-read assemblies with high BUSCO values. On the other hand, BUSCO seems to be limited by the sequencing errors introduced by PacBio in the identification of gene models (Watson and Warr 2019). Even with multiple rounds of error correction, BUSCO fails to recognize genes that are actually present, at least partially, in the assembly (Watson and Warr 2019). Moreover, BUSCO seems to be trained and based on a set of core genes identified from Sanger and Illumina assemblies. As such, BUSCO does not quantify genes in PacBio assemblies that were previously missing in Illumina genomes, which would be needed for a fair genome completeness comparison. This tendency is also evident from our results: for example after gap-filling lycPyrIL with long reads, 10 genes were not detectable anymore in the resulting assembly lycPyrILPB (**Supplementary Table S2**). A similar dynamic was observed also during the assembly process of the superb fairy-wren *Malarus cyaneus* (Peñalba et al. 2019) where BUSCO values dropped with long-read gap-filling but were restored after sequence polishing.

The new technologies have the potential to assemble very repetitive regions (e.g. MHC) and elusive chromosomes (e.g., W and microchromosomes). For this reason, quality assessment should rely upon measuring the efficiency in assembling difficult regions and not on those regions that we already obtain with previous technologies. We therefore decided to measure genome completeness and quality by characterising and quantifying repetitive regions.

Long reads were instrumental, not only to find and mask more repeats, but also to assemble and discover previously overlooked repetitive sequences. In fact, by adding PacBio sequence data we were able to significantly increase the number of predicted repeat subfamilies compared to the repeat library previously built on three birds-of-paradise species (from 112 to 183 consensus

sequences; Prost et al. (2019)). These 71 new consensus sequences were only predicted by RepeatModeler using the PacBio assembly, probably because the respective repeats were too fragmented or assembled in too few copies in Illumina assemblies. A clear example is given by the satellite DNA repeats that are severely depleted from both the lycPyrIL assembly (**Figure 3e-f**, **Figure4b**) and from the previous repeat library. With our new repeat library we could increase the base pairs masked by RepeatMasker by up to 38 % within the same assembly (lycPyr6). This indicates that while longer read lengths are important for assembling repeats, only with a comprehensive repeat library we can quantify their actual efficiency.

Repetitive elements are not only made up of transposable elements and satellite repeats, but also of multi-copy genes. One of the most repetitive gene family is the Major Histocompatibility Complex (MHC) involved in the adaptive immune response. In birds, MHC genes are located on one of the most difficult chromosomes to assemble, namely chromosome 16 (Miller and Taylor 2016). We recovered several scaffolds from this chromosome for which the only, though fragmented, assembly exists from chicken (Warren et al. 2017). We counted how many MHC IIB copies we could retrieve in the different assemblies, using BLAST hits to exon 2 and 3 sequences as proxy. We found the maximum number of copies in lycPyrPB (**Figure 3g-h**) followed by lycPyr6, suggesting that the misassembly correction with the CHiCAGO map affected the MHC genes, with the number of hits of exon 2 decreasing and for exon 3 increasing. Short-read assemblies harbour fewer MHC IIB exon copies but we note that 10XGenomics could assemble a couple more copies compared to standard Illumina data. Moreover, lycPyrSN1 contained slightly more MHC genes than lycPyrSN2 assembled with longer input molecule length.

As a further use of repetitive elements as quality measures, we tested the LTR Assembly Index (LAI; Ou et al. (2018)) that assesses the quality of an assembly from the completeness of the LTR retrotransposons present. It was not possible to obtain values for the Illumina and 10XGenomics

assemblies because the tool requires a certain baseline quantity of the full-length LTR assembled to run as initial requirements. Nonetheless, both lycPyrPB and lycPyr6 show LAI scores (respectively 11.89 and 13.59, **Supplementary Table S3**, **Supplementary Figure S1**) typical for high-quality reference genomes (as indicated in Ou et al. (2018)) and higher than those of chicken (**Supplementary Figure S2**). The increase in LAI value from lycPyrPB and lycPyr6 indicates that the assembly curation process, mostly gap-filling and polishing, improved the quality of the primary assembly.

In addition to repetitive elements, base composition is the other main factor that limits completing genome assemblies. We thus assessed the GC-content per window for each assembly (**Figure 3b**, **Supplementary Figure S7**) and as expected, found more GC-rich windows in lycPyrPB compared to the other *de-novo* assemblies (**Supplementary Figure S7**). High GC-content is often associated with non-B DNA structures like G4 that have been shown to introduce sequencing errors during polymerisation (Guiblet et al. 2018). We predicted the presence of G4 motifs in our assemblies (**Figure 3c**) and Illumina and 10XGenomics assemblies have about 1.6-2.6 Mb less of G4 compared to lycPyrPB. In this case, linked reads did not help to get a more complete overview of this genomic feature respect to regular Illumina libraries. On the other hand, the overall curation from lycPyrPB to lycPyr6 improved G4 prediction. G4 structures influence various molecular mechanisms such as alternative splicing and recombination, therefore more complete assemblies make these regions accessible for comparative genomic analysis.

Strengths and limitations of sequencing technologies

Nowadays, we have a plethora of sequencing technologies to choose from, each with their own advantages and limitations. On top of that, the large number of assembly tools available and hundreds of parameters to tweak makes it inevitable to produce numerous different assembly versions. For example, we generated 15 different assemblies only for the parameter optimization of

677 the linked-read scaffolding (**Figure 1d**) and there are studies generating even 400 assemblies in
678 total (Montoliu-Nerin et al. 2019). In such a situation, it might seem difficult to decide how to
679 choose the "best" assembly among dozens. Here we present what we learned from the different
680 technologies and how they help in resolving the genomic regions that are most difficult to assemble.
681
682 We used two types of *de-novo* assemblies based on Illumina sequencing. The first, lycPyrIL is an
683 Illumina assembly made from multiple insert size libraries of paired end and mate pair reads (Prost
684 et al. 2019); the second on 10XGenomics linked reads (lycPyrSN1 and SN2). It is notable that
685 lycPyrIL is much more contiguous than lycPyrSN1 and SN2 (contig N50 of 620 kb vs 145-150 kb;
686 **Table 1**) and has much fewer gaps. Although lycPyrIL is a less fragmented assembly, lycPyrSN2
687 has a better resolution for repeats since 7 Mb more repeats are masked and a larger number of MHC
688 IIB exons are present (**Figure3g-h**) as well as G4 motifs (**Figure 3g**). Nonetheless, the contiguity
689 reached in lycPyrPB for the same sample at contig level (contig N50 of 6 Mb) is ten-fold higher
690 than in lycPyrIL and even outscores lycPyrIL scaffold N50 of 4 Mb. 10XGenomics linked reads
691 bring long-range information through the barcode system that is useful for local phasing, detection
692 of structural variations (Zheng et al. 2016; Marks et al. 2019), scaffolding (Yeo et al. 2017) and
693 construction of recombination maps (Dréau et al. 2019; Sun et al. 2019). We used the barcode
694 information to scaffold the PacBio assembly (lycPyr3, **Table 1**) without obtaining many new
695 scaffolds but this could be due to the already high contiguity of the input lycPyrPB assembly.
696 Finally, we note that the molecule input length for the 10XGenomics libraries have different effects
697 on the assembly and BUSCO scores. That is, lycPyrSN1 (24 kb mean molecule length library)
698 outscores lycPyrSN2 (26.1 kb mean molecule length library) in the number of complete BUSCO
699 genes (**Supplementary Table S2**). Even though 10XGenomics linked reads consist of short reads,
700 both lycPyrSN1 and lycPyrSN2 have more missing genes compared to lycPyrIL (**Supplementary**
701 **Table S2**).
702

Long reads together with proximity ligation maps are game changers in genomics. Their combination yielded a very high-quality assembly for a non-model bird with suboptimal sample quality (see mean molecule lengths for 10XGenomics assemblies above). The PacBio assembly is by far the most contiguous and a suitable genomic backbone to obtain chromosome models including the W chromosome and several microchromosomes. The main weakness linked to PacBio is the introduction of sequencing errors (mostly short indels) that must be corrected with accurate short reads. As mentioned before, the sequencing errors hinder the identification of gene models (BUSCO) and protein prediction (Watson and Warr 2019). Moreover, the PacBio assembly is likely not free of misassemblies (e.g., chimeric contigs). Thus a second type of independent data is necessary to detect such errors; e.g., ~100 potential misassemblies were identified by the CHiCAGO proximity map. The CHiCAGO map was very useful to correct the assembly and make a first scaffolding, but neither alone nor with 10XGenomics scaffolding yielded a chromosome-level assembly. The only type of data implemented here that allowed the generation of chromosome models was the Hi-C map. The latter does not rely on extracted DNA quality or library insert size, but instead on *in-situ* proximity within the nuclei of the fixed sample. As such, Hi-C data is an effective replacement of linkage maps for scaffolding purposes (Dudchenko et al. 2017) and can be used to manually curate assemblies.

A direct way to identify the limits of sequencing data is to investigate where assemblers fail to resolve sequences, i.e. where contig fragmentation occurs. Therefore, we characterized what causes contig fragmentation in each assembly by analysing sequences directly adjacent to gaps and inferring the gap content of draft assemblies by aligning their flanks to the final multiplatform version lycPyr6 (**Figure 4a**). In general, we found that long and/or homogeneous repeats such as LTR retrotransposons, satellites, and simple repeats are the main fragmentation causes in every assembly, though the specific repeat type changed with the technology. Short-read and linked-read contigs mostly break at simple repeats. Even though the percentage of simple repeats assembled in

lycPyrIL, lycPyrSN1 and lycPyrSN2 ranges between 80-90% relative to lycPyr6 (**Figure 4b**), simple repeats also caused most of the assembly gaps, indicating that insert size and linked read methods are not sufficient to unambiguously solve those regions (**Figure 4c-d**). At the same time, the gaps of these three assemblies, when compared to the final multiplatform assembly, mainly contain LTR retrotransposons, simple repeats and complex repeats (defined as arrays of different types of repeats; **Figure 4e-f**). LTR retrotransposons are the second most abundant retrotransposons in the paradise crow assembly and several kilobases long. These features make LTR retrotransposons the major cause of fragmentation in the PacBio assembly and the second in the short-read ones. This partially unexpected trend is likely because LTR retrotransposons are underrepresented in lycPyrIL, lycPyr SN1 and lycPyrSN2 (as indicated by their lack of part of the recent LTR activity; **Figure 3e-f**). The same pattern can be observed for the multicopy rRNA genes: the only assemblies showing gaps caused by rRNA genes are the PacBio-based and this is likely because PacBio was the only technology able to (partially) solve those repeats (**Figure 4c-d**). It is interesting that linked reads appear to better distinguish long repeats like LTR retrotransposons than short-read libraries based on insert size (**Figure 4b**). The satellite portion of the genome was significantly better assembled with PacBio long reads (~9 Mb), while neither multiple Illumina libraries nor linked reads could assemble more than 1 Mb of satellites. This is probably due to the highly homogeneous nature of long stretches of satellites that make satellite arrays collapse during assembly (Hartley and O'Neill 2019). Similar to LTR retrotransposons and rRNA genes, satellites are barely assembled in lycPyrIL, lycPyrSN1 and lycPyrSN2. Therefore satellites are not a major cause of contig fragmentation in Illumina-based assemblies. LINEs are usually short retrotransposons due to 5' truncation during integration (Levin and Moran 2011)and in the paradise crow and other songbirds they seem to be mostly present in old copies (**Figure 3e**; Suh et al. (2018); Weissensteiner et al. (2019)). Therefore they likely are less homogeneous elements, with more diagnostic mutations and hence easier to assemble. In fact, both Illumina and 10XGenomics assemblies have 96-98% of LINEs assembled and LINEs represent only the fourth causative factor

of fragmentation. Finally, we noticed a disproportion of DNA transposons annotated in the Illumina assemblies (lycPyrIL and lycPyrILPB) compared to the other assemblies. This phenomenon might be explained by annotation issues linked to the fragmentation of those regions or by the presence of unsolved haplotypes. DNA transposons have been inactive in songbirds for even longer than LINEs (Kapusta and Suh 2017) and should thus be rather straightforward to assemble.

Conclusions

Thanks to a manually curated multiplatform assembly and three *de-novo* draft assemblies for the same sample, we were able to characterise and measure genome completeness across sequencing technologies. As expected, long-read assemblies are more complete than short-read assemblies but completeness has been usually measured with statistics that are optimized for short reads rather than for long reads. Scaffold N50 and BUSCO values do not reflect the entire potential and strengths of new sequence technologies, therefore we measured completeness focusing on the most difficult-to-assemble genomic regions. By doing so, we traced the essential steps for generating a high-quality assembly for a non-model organism while optimizing costs and efforts.

Based on our assembly comparisons, the essential elements to make a chromosome-level assembly are a contiguous primary assembly based on long reads, an independent set of data for correcting misassemblies (CHiCAGO map or linked reads) and polish sequencing errors (short or linked reads), and a Hi-C map for chromosome-level scaffolding. PacBio needs error correction both at the nucleotide level (base calling errors and short indels) and at the assembly level (e.g., chimeric contigs). For both scopes it is possible to use Illumina data but a note of caution is due. First, when polishing the assembly for base calling errors and short indels, short reads could over-homogenize repetitive sequences and thus it would be advisable to correct only outside repeats. In addition, 10XGenomics linked reads can also be used to correct both sequencing errors and misassemblies (e.g., Tigmint, Jackman et al. (2018)) and to scaffold the genome (ARCS, Yeo et al. (2017), ARKS,

781 Coombe et al. (2018), fragScaff, Adey et al. (2014)). In general, the spatial information brought by
782 linked reads seems to be very versatile (e.g., assembly correction, scaffolding, structural variation
783 inference, haplotype phasing) and able to better avoid over-collapsing of repetitive elements and
784 genes (**Figure 3** and **4**). Therefore, if budgets and sample material are limited, this technology may
785 be suitable to obtain a better genomic overview than short reads alone. Nevertheless, long reads
786 provide the most detailed look into difficult-to-assemble genomic regions. We summarized the
787 strengths and limitations of the implemented technologies in **Figure 5** that can be used as a guide
788 for choosing technologies and ranking assemblies.

789

790 We have shown that recent technological developments have led to enormous improvements in
791 assembly quality and completeness, paving the way to more complete comparative genomic analyses,
792 including regions that were previously inaccessible within genomic dark matter. At the same time,
793 awareness of technological strengths and weaknesses in resolving repeat-rich and GC-rich regions is
794 fundamental for choosing the most suitable technology when designing sequencing projects, and will
795 help in a dilemma many genome scientists face these days: choosing the best assembly among many.

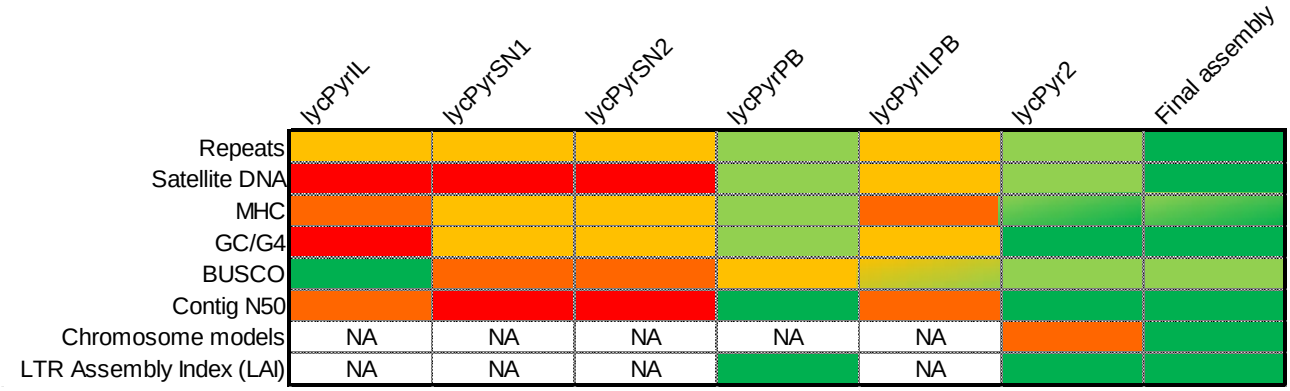

796

797 **Figure 5**. Summary of the relative efficiency of the different technologies over
798 quality/completeness parameters. Green: most effective; red: least effective.

799

800

Methods

Samples

We used pectoral muscle samples from three vouchered specimens of *Lycocorax pyrrhopterus* ssp. *obiensis* collected on Obi Island (Moluccas, Indonesia) in 2013, from the Museum Zoologicum Bogoriense (MZB) in Bogor, Indonesia, temporarily on loan at the Natural History Museum of Denmark. One female (voucher: MZB 34.073) sample preserved in DMSO was used for PacBio, Illumina and 10XGenomics sequencing and for the Dovetail CHiCAGO library, one female sample (voucher: MZB 34.070) preserved in RNAlater was used for the Hi-C library with Phase Genomics, and one male sample preserved in DMSO (voucher: MZB 34.075) was used for Illumina sequencing.

Sequencing technologies and *de-novo* assemblies

We sequenced the female sample MZB 34.073 using a) PacBio RSII C6-P4 (mean of 11 kb and N50 of 16 kb for read length) for a total coverage of 72X; b) 10XGenomics with a HiSeqX Illumina machine (24 kb mean molecule length, 280 bp library insert size, 150 bp read length, net coverage 39.7X); c) 10XGenomics with HiSeqX Illumina machine (26.1 kb mean molecule length, 280 bp library insert size, 150 bp read length, net coverage 37.9X). DNA was extracted using magnetic beads on a Kingfisher robot, except for library c) which was based on DNA extracted with agarose gel plugs as in (Weissensteiner et al. 2017). In addition to these libraries, we also used the Illumina libraries and assembly produced in (Prost et al. 2019): Illumina HiSeq 2500 TruSeq paired-end libraries (180 bp and 550 bp insert sizes) and Nextera mate pair libraries (5 kb and 8 kb insert sizes) for a total coverage of 90X. Furthermore, two paired-end libraries (125 bp read length) of chromatin-chromatin interactions from CHiCAGO and Hi-C techniques were produced using a HiSeq 2500 by Dovetail Genomics (Putnam et al. 2016) and Phase Genomics (more details below), respectively. Finally, we generated a paired-end library with insert size of 650 bp on an Illumina HiSeqX machine for the male sample.

For each library/technology (namely Illumina, 10XGenomics and PacBio) we made independent *de-novo* assemblies. (Prost et al. 2019) used ALLPATHS-LG (Butler et al. 2008) for Illumina data while we used Falcon (Chin et al. 2016) for PacBio data and Supernova2 (Weisenfeld et al. 2017) for 10XGenomics data (**Table 1**). All the basic genome statistics of the assemblies (**Supplementary Table S1**) were calculated using the Perl script assemblathon_stats.pl from https://github.com/KorfLab/Assemblathon/blob/master/assemblathon_stats.pl.

Identification of sex-linked contigs and PAR

Given the extreme conservation of the Z chromosomes of songbird (Xu et al. 2019), we used the Z-chromosome sequence of great tit as a query to search for homologous Z-linked contigs in paradise crow. The aligner nucmer was used to perform the one-to-one alignment of the great tit genome and lycPyrPB. Those contigs with more than 60 percent sequence aligned to great tit Z chromosome were identified as Z-linked. We further calculated the sequencing coverage using the female Illumina paired-end libraries to confirm the half-coverage pattern of candidate Z-linked contigs relative to autosomal contigs. We used BWA-MEM to map the reads and the samtools depth function to estimate contig coverage. To identify candidate W-linked contigs, we calculated the re-sequencing coverage of the male individual, because W-linked contigs are female-specific and are not expected to be mapped by male reads while the coverage of female reads should be half of that of autosomes. We used the known PAR sequences of collared flycatcher (Smeds et al. 2014) to identify the homologous PAR contigs in paradise crow. As expected, the PAR contigs were found to show similar re-sequencing coverage in both the male and the female as on the autosomes.

Multiplatform approach

We created three types of multiplatform assemblies, one that combines only Illumina and PacBio data (lycPyrILPB, see **Table 1**), a second one combining PacBio and Hi-C data, and a third more

851 comprehensive one that combines three types of sequencing data and two types of proximity ligation
852 data (lycPyr6).
853
854 For the first type of assembly (lycPyrILPB), we used the Illumina assembly lycPyrIL (Prost et al.
855 2019) as genomic backbone and gap-filled it with PacBio long reads using the software PBJelly
856 (PBSuite v. 15.8.24) maintaining the all the default options but -min 10 to consider only gaps of at
857 least 10 base pairs length. The second multiplatform assembly lycPyrHiC was built by scaffolding
858 the PacBio primary assembly (lycPyrPB) with Hi-C data.
859
860 For the most comprehensive assembly (lycPyr6), we combined PacBio, Illumina, 10XGenomics,
861 CHiCAGO and Hi-C data (**Figure 1**). The first step was to assemble the PacBio reads into a primary
862 assembly with the Falcon software (Chin et al. (2016); **Figure 1a**). The primary contigs were
863 corrected and scaffolded with the Dovetail CHiCAGO map generating lycPyr2 (**Figure 1b**) using the
864 software HiRise (Putnam et al. 2016). lycPyr2 then was polished with long reads (two runs of Arrow;
865 Chin et al. (2016)) and short reads (three runs of Pilon 1.22; Walker et al. (2014); **Figure 1c**). Since
866 PacBio sequencing is prone to introduce short indels in the reads (Eid et al. 2009), we addressed
867 specifically these sequencing problems with Pilon while we did not correct single nucleotide variants.
868 Furthermore, in order to not over-polish repetitive regions (i.e., homogenising them with short reads),
869 we excluded Pilon corrections falling within repeats identified by RepeatMasker 4.0.7 using our
870 custom repeat library.
871
872 We then scaffolded lycPyr2 using the long-range information given by 10XGenomics linked reads
873 with the software ARCS 1.0.1 (Yeo et al. (2017); parameters -s 95 -e 1000 -m 20-100000) and LINKS
874 1.8.5 (Warren et al. (2015); parameters -a 0.2) generating lycPyr3 (**Figure 1d**). The parameters for
875 ARCS and LINKS have been chosen after generating 15 assemblies with different values for -m -e -
876 a (**Supplementary Table S11**). The optimal parameter combination was established by minimising

a) the number of "private" scaffolds belonging only to one combination of parameters, b) the number of scaffolds containing putative in-silico chromosomal translocations.

lycPyr3 was scaffolded into chromosome models (clusters of contigs and scaffolds) with the Phase Genomics Hi-C data and the Proximo Hi-C scaffolding pipeline (lycPyr4; **Figure 1e**). Hi-C data were generated using a Phase Genomics (Seattle, WA) Proximo Hi-C Animal Kit. Following the manufacturer's instructions for the kit, intact cells from two samples were crosslinked using a formaldehyde solution, digested using the Sau3AI restriction enzyme, and proximity ligated with biotinylated nucleotides to create chimeric molecules composed of fragments from different regions of the genome that were physically proximal *in-vivo*, but not necessarily linearly proximal. Continuing with the manufacturer's protocol, molecules were pulled down with streptavidin beads and processed into an Illumina-compatible sequencing library.

Reads were aligned to the draft assembly lycPyr3 following the manufacturer's recommendations. Briefly, reads were aligned using BWA-MEM (Li and Durbin (2010); v. 0.7.15-r1144-dirty) with the -5SP and -t 8 options specified, while keeping the other parameters as default. SAMBLASTER (Faust and Hall 2014) was used to flag PCR duplicates, which were later excluded from analysis. Alignments were then filtered with samtools (Li et al. (2009); v1.5, with htslib 1.5) using the -F 2304 filtering flag to remove non-primary and secondary alignments, as well as read pairs in which one or more mates were unmapped. Phase Genomics' Proximo Hi-C genome scaffolding platform was used to create chromosome-scale scaffolds from the draft assembly as described in (Bickhart et al. 2017). As in the LACHESIS method (Burton et al. 2013), this process computes a contact frequency matrix from the aligned Hi-C read pairs, normalised by the number of Sau3AI restriction sites (GATC) on each contig, and constructs scaffolds in such a way as to optimise expected contact frequency and other statistical patterns in Hi-C data. Approximately 286,000 separate Proximo runs were performed

to optimise the number of scaffolds and scaffold construction in order to make the scaffolds as concordant with the observed Hi-C data as possible.

Two chromosomes (chr1 and chr2) appeared to be split into two different super-scaffolds (or clusters) respectively, thus they were manually put together following the orientation suggested by the Hi-C interaction heatmap (**Supplementary Figure S3**). We then manually inspected the assembly lycPyr4 for misassemblies (**Figure 1f** and **Figure 2**) by aligning the four *de-novo* assemblies (lycPyrIL, lycPyrPB, lycPyrSN1 and lycPyrSN2) to it using Satsuma2 (Grabherr et al. 2010) and chromosome models from three songbird outgroups (*Ficedula albicollis*, *Taeniopygia guttata* and *Parus major*) with LASTZ 1.04.00 (Harris 2007). We identified misassemblies by looking for regions in which the different *de-novo* assemblies were in conflict with the final assembly (schematically showed in **Figure 2**). We applied the majority rule for each scaffolding or orientation conflict found between lycPyr4 and the four draft assemblies. To make any decisions against the scaffold configuration in lycPyr4, three of the four *de-novo* assemblies needed to be in discordance with lycPyr4 and show the same pattern of discordance. In cases where only two *de-novo* assemblies showed the same pattern of discordance and the other were not informative, we used the information provided by the outgroups to decide whether to keep the lycPyr4 scaffold configuration or correct it. With this approach we were able to identify 45 intra-scaffold misassemblies at a fine scale, all of them being orientation issues of PacBio contigs within scaffolds.

Then, we gap-filled the assembly using PBJelly (PBSuite 15.8.24; English et al. (2012)) with the default options except for the parameter -min 10 in order to consider the gaps longer than 10 bps (**Figure 1g**). After the gap-filling step that used the PacBio reads, we ultimately polished the genome with long reads using Arrow (one run; PacBio library) and with short reads using Pilon (two runs; Illumina library; **Figure 1h**).

The last step of assembly curation involved the generation of Hi-C heatmaps on lycPyr5 by mapping the Hi-C library to the assembly using Juicer 1.5 (Durand et al. (2016); **Figure 1i**). We manually inspected the Hi-C maps for misassemblies using Juicebox 1.9.8 (https://github.com/aidenlab/Juicebox) and corrected lycPyr5 accordingly (**Supplementary Figure S3**). This way, we manually solved remaining assembly issues regarding the orientation and order of some contigs or scaffolds within the chromosome models, as well as corrected *in-silico* chromosomal translocations.

The completeness of the assemblies was assessed with gVolante (Nishimura et al. 2017) using BUSCO v3 for avian genomes (**Supplementary Table S2**) and with LTR Assembly Index (Ou et al. (2018); **Supplementary Table S3**).

The mitochondrial genome was identified as one PacBio contig by aligning the mtDNA of *Corvus corax* (GenBank accession number KX245138.1) to lycPyrPB. It was annotated using DOGMA (Wyman et al. 2004) and tRNAscan-SE 1.3.1 (Lowe and Eddy (1997); **Supplementary Table S12**).

Chromosome nomenclature

Since the chicken genome is the best avian genome assembled so far with reliable chromosome information (Warren et al. 2017), we named and oriented our chromosome models according to homology with galGal5 (RefSeq accession number GCF_000002315.6). In the case that our chromosome models were not completely collinear with chicken, we oriented them following the orientation of the majority of the model respect to chicken. Finally, if the chromosome models did not share any homology with chicken, their orientation was not changed.

Repeat library

We produced a *de-novo* repeat library for paradise crow by running the RepeatMasker 4.0.7 and RepeatModeler 1.0.8 software on the PacBio *de-novo* assembly. We hard-masked lycPyrPB with the Aves repeat library from Repbase (version 20170127; https://www.girinst.org/about/repbase.html) together with the consensus sequences from (Prost et al. 2019), then ran RepeatModeler. The new consensus sequences generated by RepeatModeler were aligned back to the reference genome; the 20 best BLASTN 2.7.1+ results were collected, extended by 2 kb on both sides and aligned to one another with MAFFT 7.4.07. The alignments were manually curated applying the majority rule and the superfamily of repeat assessed following the (Wicker et al. 2007) classification.

All the new consensus sequences were masked in CENSOR (http://www.girinst.org/censor/index.php) and named according to homology to known repeats in the Repbase database. Sequences with high similarity to known repeats for their entire lengths were given the name of the known repeat + suffix "_lycPyr"; repeats with partial homology have been named with the suffix "-L_lycPyr" where "L" stands for "like" (Suh et al. 2018). Repeats with no homology with known ones have been considered as new families and named with the prefix "lycPyr" followed by the name of their superfamilies.

The final repeat library also contains the manually curated version of the consensus sequences previously generated on other two birds-of-paradise *Astrapia rothschildi* "astRot", *Ptiloris paradiseus* "ptiPar" (Prost et al. 2019), the ones from *Corvus cornix* (Weissensteiner et al. 2019), *Uraeginthus cyanocephalus* (Boman et al. 2019), *Ficedula albicollis* and all the avian repeats available on Repbase (mostly from chicken and zebra finch).

G4 motif identification

The *de-novo* assemblies and the final version have been scanned for G-quadruplex (G4) motifs with the software Quadron (Sahakyan et al. (2017); https://github.com/aleksahak/Quadron). Only non-

978 overlapping hits with a score greater than 19 were used for subsequent analysis as suggested in
979 (Sahakyan et al. 2017). The density of such motifs per chromosome model was calculated using
980 bedtools coverage (BEDTools 2.27.1; Quinlan (2014)).
981
982 **MHC class IIB analysis**
983 To infer how highly duplicated genes are assembled with different input data and assembly
984 strategies, we investigated the distribution of major histocompatibility class IIB (MHCIIB)
985 sequence hits in seven assemblies: lycPyrIL, lycPyrPB, lycPyrSN1, lycPyrSN1, lycPyrILPB,
986 lycPyr2 and lycPyr6 (the intermediate assemblies like lycPyr3 are not shown here because the MHC
987 content did not change from lycPyr2 to lycPyr5). We performed BLAST (Altschul et al. 1990)
988 searches both with sequences of the highly variable exon 2 that encodes the peptide binding region,
989 and with the much more conserved exon 3 (Hughes and Yeager 1998), as the disparate levels of
990 polymorphism within these regions may provide insights into different aspects of challenges with
991 genome assembly. We conducted tBLASTn (BLAST 2.7.1+) searches using alignments available
992 from Goebel et al. (2017) that include sequences from across the entire avian phylogeny. We chose
993 this strategy to ensure the identification MHCIIB sequences, as with sequences of only a single-
994 species BLAST search might miss highly divergent sequences as they are often present in the MHC,
995 where within-species diversity of MHC genes often equals between-species divergence. From the
996 available alignments, we exclusively retained sequences spanning the entire 270 bp of exon 2 and
997 sequences covering 220 bp of exon 3. This left query alignments including 233 sequences from 22
998 bird orders/families for exon 2, and 314 sequences from 26 bird orders/families for exon 3.
999 Overlapping blast hit intervals were merged. To ensure that these intervals contained sequences
1000 corresponding to MHCIIB, we first BLAST searched them back against the GenBank database
1001 using BLASTn queries, and retained only intervals producing hits with MHCIIB. We then aligned
1002 the remaining sequences using the MAFFT alignment server with the --add option and default
1003 settings, and manually screened the alignments to identify non-MHCIIB sequences. Finally, we

1004 determined the alignment lengths of BLAST hit intervals after removing insertions relative to the
1005 query alignment. We report only hits longer than 240 bp for exon 2 and longer than 195 bp for exon
1006 3, corresponding to approximately 90% of the respective query alignment lengths.
1007
1008 **Gap analysis**
1009 For each assembly produced, we estimated the number of gaps caused by repeats by intersecting the
1010 gap and repeat coordinates using bedtools window (Quinlan 2014) with a window size of 100 bp
1011 (**Figure 4a**). Only gaps longer than 10 bp were taken into consideration. This filter is particularly
1012 important for lycPyrIL since there are many small gaps of 1-5 Ns that are probably caused by
1013 sequencing or base-calling errors.
1014
1015 We estimated what is missing in the draft assemblies with respect to the final multiplatform assembly
1016 lycPyr6 by aligning the flanking regions to the gaps onto the final version. We then assessed the
1017 presence of annotated repeats on lycPyr6 between the aligned flanking regions to the draft assembly
1018 gaps. To do these pairwise alignments, we extracted 500 bp of flanking regions from the intra-scaffold
1019 gaps of lycPyrIL, lycPyrSN1, lycPyrSN2, lycPyrPB and lycPyrILPB and BLASTn searched the
1020 sequences to lycPyr6 with BLAST 2.7.1+. The alignments were filtered to retain only unambiguously
1021 orthologous positions on lycPyr6, namely there was only one alignment (98% identity, 90% coverage)
1022 of both flanks on the same lycPyr6 scaffold. The coordinates of the draft genome gaps projected onto
1023 lycPyr6 were then intersected with the RepeatMasker annotation using bedtools intersect. Draft
1024 genome gaps containing only one type of repeat on lycPyr6 were classified according to the type of
1025 repeat. In case the draft genome gaps corresponded to a region containing more than one type of
1026 repeat, the gaps were classified as 'complex'. Finally, in case that the draft genome gaps could not be
1027 mapped unambiguously (e.g., no homology, only one flank aligned or the two flanking regions
1028 mapped to different scaffolds) or mapped to gaps on lycPyr6, they were classified as 'not scorable
1029 gaps' (**Figure 4a**)

We also compared how many repeats were assembled in the draft assemblies compared to lycPyr6 (**Figure 4b**) by calculating the proportion of repeat base pairs present in the draft assemblies relative to the total bp in lycPyr6. This was done for each major repeat group using the RepeatMasker table (.tbl) files; more details in **Supplementary Table S10**.

Data Access

Acknowledgements

We would like to thank Max Käller, Phil Ewels, Remi-André Olsen, Joel Gruselius, Fanny Taborsak-Lines (SciLifeLab Stockholm) for generating 10X data; Olga Vinnere-Pettersson and Ida Höijer (SciLifeLab Uppsala) for generating PacBio data; Mai-Britt Mosbech and Anna Petri (SciLifeLab Uppsala) for doing the agarose gel plug extraction; Verena Kutschera at the National Bioinformatics Infrastructure Sweden at SciLifeLab (Stockholm) for bioinformatics advice; Muhammad Bilal for the help with the repeat library; Matthias Weissensteiner for the help with sample transfer, comments on the manuscript and helpful discussions; Douglas Scofield for help with the gap-filling analysis; Diem Nguyen, Marco Ricci, James Galbraith, Julie Blommaert, Ivar Westerberg, Jesper Boman for their comments on the manuscript; Octavio Gimenez-Palacio, David Adelson, James Galbraith, Hanna Johannesson, Jesper Boman, and Boel Olsson for helpful discussions. This research was supported by grants from the Swedish Research Council Formas (2017-01597 to AS), the Swedish Research Council Vetenskapsrådet (2016-05139 to AS, and 621-2014-5113 to MI), and the SciLifeLab Swedish Biodiversity Program (2015-R14 to AS). The Swedish Biodiversity Program has been made available by support from the Knut and Alice Wallenberg Foundation. A.S. acknowledges funding from the Knut and Alice Wallenberg Foundation via Hans Ellegren. The authors acknowledge support from the National Genomics Infrastructure (NGI)/Uppsala Genome Center. The work performed at NGI / Uppsala Genome Center has been funded by RFI/VR and Science for Life Laboratory, Sweden. The authors further acknowledge support from the National Genomics Infrastructure in Stockholm funded by Science for Life Laboratory, the Knut and Alice Wallenberg Foundation and the Swedish

Research Council. Some of the computations were performed on resources provided by the Swedish National Infrastructure for Computing (SNIC) through Uppsala Multidisciplinary Center for Advanced Computational Science (UPPMAX). KAJ is most grateful for the financial support received from the Villum Foundation (Young Investigator Programme, project no. 15560), and from the Carlsberg Foundation (Distinguished Associate Professor Fellowship, project no. CF17-0248). We thank the State Ministry of Research and Technology (RISTEK); the Ministry of Forestry, Republic of Indonesia; the Research Center for Biology, Indonesian Institute of Sciences (RCB-LIPI); and the Bogor Zoological Museum (Tri Haryoko) for providing permits to carry out fieldwork in Indonesia and to export select samples. KAJ acknowledges a National Geographic Research and Exploration Grant (8853-10), the Dybron Hoffs Foundation and the Corrit Foundation for financial support for fieldwork in Indonesia.

Disclosure declaration

Shawn Sullivan and Ivan Liachko are employed at Phase Genomics.

References

Adey A, Kitzman JO, Burton JN, Daza R, Kumar A, Christiansen L, Ronaghi M, Amini S, L. Gunderson K, Steemers FJ et al. 2014. In vitro, long-range sequence information for de novo genome assembly via transposase contiguity. *Genome Research* **24**: 2041-2049.

Aird D, Ross MG, Chen WS, Danielsson M, Fennell T, Russ C, Jaffe DB, Nusbaum C, Gnirke A. 2011. Analyzing and minimizing PCR amplification bias in Illumina sequencing libraries. *Genome Biol* **12**.

Alkan C, Sajjadian S, Eichler EE. 2010. Limitations of next-generation genome sequence assembly. *Nature Methods* **8**: 61.

Altschul SF, Gish W, Miller W, Myers EW, Lipman DJ. 1990. Basic local alignment search tool. *Journal of Molecular Biology* **215**: 403-410.

Bellott DW, Skaletsky H, Cho T-J, Brown L, Locke D, Chen N, Galkina S, Pyntikova T, Koutseva N, Graves T et al. 2017. Avian W and mammalian Y chromosomes convergently retained dosage-sensitive regulators. *Nature Genetics* **49**: 387.

Belser C, Istace B, Denis E, Dubarry M, Baurens F-C, Falentin C, Genete M, Berrabah W, Chèvre A-M, Delourme R et al. 2018. Chromosome-scale assemblies of plant genomes using nanopore long reads and optical maps. *Nature Plants* **4**: 879-887.

Bickhart DM, Rosen BD, Koren S, Sayre BL, Hastie AR, Chan S, Lee J, Lam ET, Liachko I, Sullivan ST et al. 2017. Single-molecule sequencing and chromatin conformation capture enable de novo reference assembly of the domestic goat genome. *Nature Genetics* **49**: 643.

Biffi G, Tannahill D, Balasubramanian S. 2012. An Intramolecular G-Quadruplex Structure Is Required for Binding of Telomeric Repeat-Containing RNA to the Telomeric Protein TRF2. *Journal of the American Chemical Society* **134**: 11974-11976.

Boman J, Frankl-Vilches C, da Silva dos Santos M, de Oliveira EHC, Gahr M, Suh A. 2019. The Genome of Blue-Capped Cordon-Bleu Uncovers Hidden Diversity of LTR Retrotransposons in Zebra Finch. *Genes* **10**: 301.

Botero-Castro F, Figuet E, Tilak M-K, Nabholz B, Galtier N. 2017. Avian Genomes Revisited: Hidden Genes Uncovered and the Rates versus Traits Paradox in Birds. *Molecular Biology and Evolution* **34**: 3123-3131.

Bourque G, Burns KH, Gehring M, Gorbunova V, Seluanov A, Hammell M, Imbeault M, Izsvák Z, Levin HL, Macfarlan TS et al. 2018. Ten things you should know about transposable elements. *Genome Biology* **19**: 199.

Burt DW. 2002. Origin and evolution of avian microchromosomes. *Cytogenetic and Genome Research* **96**: 97-112.

Burton JN, Adey A, Patwardhan RP, Qiu R, Kitzman JO, Shendure J. 2013. Chromosome-scale scaffolding of de novo genome assemblies based on chromatin interactions. *Nature Biotechnology* **31**: 1119.

Butler J, MacCallum I, Kleber M, Shlyakhter IA, Belmonte MK, Lander ES, Nusbaum C, Jaffe DB. 2008. ALLPATHS: De novo assembly of whole-genome shotgun microreads. *Genome Research* **18**: 810-820.

Chaisson MJP, Huddleston J, Dennis MY, Sudmant PH, Malig M, Hormozdiari F, Antonacci F, Surti U, Sandstrom R, Boitano M et al. 2014. Resolving the complexity of the human genome using single-molecule sequencing. *Nature* **517**: 608.

Chaisson MJP, Wilson RK, Eichler EE. 2015. Genetic variation and the de novo assembly of human genomes. *Nature Reviews Genetics* **16**: 627.

Chalopin D, Volff J-N, Galiana D, Anderson JL, Schartl M. 2015. Transposable elements and early evolution of sex chromosomes in fish. *Chromosome Research* **23**: 545-560.

Chang C-H, Chavan A, Palladino J, Wei X, Martins NMC, Santinello B, Chen C-C, Erceg J, Beliveau BJ, Wu C-T et al. 2019. Islands of retroelements are major components of Drosophila centromeres. *PLOS Biology* **17**: e3000241.

Charlesworth B, Harvey PH, Charlesworth B, Charlesworth D. 2000. The degeneration of Y chromosomes. *Philosophical Transactions of the Royal Society of London Series B: Biological Sciences* **355**: 1563-1572.

Chin C-S, Peluso P, Sedlazeck FJ, Nattestad M, Concepcion GT, Clum A, Dunn C, O'Malley R, Figueroa-Balderas R, Morales-Cruz A et al. 2016. Phased diploid genome assembly with single-molecule real-time sequencing. *Nature Methods* **13**: 1050.

Chuong EB, Elde NC, Feschotte C. 2016. Regulatory activities of transposable elements: from conflicts to benefits. *Nature Reviews Genetics* **18**: 71.

Coombe L, Zhang J, Vandervalk BP, Chu J, Jackman SD, Birol I, Warren RL. 2018. ARKS: chromosome-scale scaffolding of human genome drafts with linked read kmers. *BMC Bioinformatics* **19**: 234.

Cowley M, Oakey RJ. 2013. Transposable Elements Re-Wire and Fine-Tune the Transcriptome. *PLOS Genetics* **9**: e1003234.

Deschamps S, Zhang Y, Llaca V, Ye L, Sanyal A, King M, May G, Lin H. 2018. A chromosome-scale assembly of the sorghum genome using nanopore sequencing and optical mapping. *Nature Communications* **9**: 4844.

Dohm JC, Lottaz C, Borodina T, Himmelbauer H. 2008. Substantial biases in ultra-short read data sets from high-throughput DNA sequencing. *Nucleic Acids Res* **36**.

Domanska D, Kanduri C, Simovski B, Sandve GK. 2018. Mind the gaps: overlooking inaccessible regions confounds statistical testing in genome analysis. *BMC Bioinformatics* **19**: 481.

Dréau A, Venu V, Avdievich E, Gaspar L, Jones FC. 2019. Genome-wide recombination map construction from single individuals using linked-read sequencing. *Nature Communications* **10**: 4309.

Du Z, Zhao Y, Li N. 2008. Genome-wide analysis reveals regulatory role of G4 DNA in gene transcription. *Genome Research* **18**: 233-241.

Du Z, Zhao Y, Li N. 2009. Genome-wide colonization of gene regulatory elements by G4 DNA motifs. *Nucleic Acids Research* **37**: 6784-6798.

Dudchenko O, Batra SS, Omer AD, Nyquist SK, Hoeger M, Durand NC, Shamim MS, Machol I, Lander ES, Aiden AP et al. 2017. De novo assembly of the *Aedes aegypti* genome using Hi-C yields chromosome-length scaffolds. *Science* **356**: 92-95.

Dudchenko O, Shamim MS, Batra SS, Durand NC, Musial NT, Mostofa R, Pham M, Glenn St Hilaire B, Yao W, Stamenova E et al. 2018. The Juicebox Assembly Tools module facilitates *de novo* assembly of mammalian genomes with chromosome-length scaffolds for under $1000. *bioRxiv* doi:10.1101/254797: 254797.

Durand NC, Shamim MS, Machol I, Rao SSP, Huntley MH, Lander ES, Aiden EL. 2016. Juicer Provides a One-Click System for Analyzing Loop-Resolution Hi-C Experiments. *Cell Systems* **3**: 95-98.

Eid J, Fehr A, Gray J, Luong K, Lyle J, Otto G, Peluso P, Rank D, Baybayan P, Bettman B et al. 2009. Real-Time DNA Sequencing from Single Polymerase Molecules. *Science* **323**: 133-138.

Emera D, Wagner GP. 2012. Transposable element recruitments in the mammalian placenta: impacts and mechanisms. *Briefings in Functional Genomics* **11**: 267-276.

English AC, Richards S, Han Y, Wang M, Vee V, Qu J, Qin X, Muzny DM, Reid JG, Worley KC et al. 2012. Mind the Gap: Upgrading Genomes with Pacific Biosciences RS Long-Read Sequencing Technology. *PLOS ONE* **7**: e47768.

Etherington GJ, Heavens D, Baker D, Lister A, McNelly R, Garcia G, Clavijo B, Macaulay I, Haerty W, Di Palma F. 2019. Sequencing smart: *De novo* sequencing and assembly approaches for non-model mammals. *bioRxiv* doi:10.1101/723890: 723890.

Faino L, Seidl MF, Datema E, van den Berg GCM, Janssen A, Wittenberg AHJ, Thomma BPHJ. 2015. Single-Molecule Real-Time Sequencing Combined with Optical Mapping Yields Completely Finished Fungal Genome. *mBio* **6**: e00936-00915.

Goebel J, Promerová M, Bonadonna F, McCoy KD, Serbielle C, Strandh M, Yannic G, Burri R, Fumagalli L. 2017. 100 million years of multigene family evolution: origin and evolution of the avian MHC class IIB. *BMC Genomics* **18**: 460.

Goodwin S, McPherson JD, McCombie WR. 2016. Coming of age: ten years of next-generation sequencing technologies. *Nature Reviews Genetics* **17**: 333.

Gordon D, Huddleston J, Chaisson MJP, Hill CM, Kronenberg ZN, Munson KM, Malig M, Raja A, Fiddes I, Hillier LW et al. 2016. Long-read sequence assembly of the gorilla genome. *Science* **352**: aae0344.

Grabherr MG, Russell P, Meyer M, Mauceli E, Alföldi J, Di Palma F, Lindblad-Toh K. 2010. Genome-wide synteny through highly sensitive sequence alignment: Satsuma. *Bioinformatics (Oxford, England)* **26**: 1145-1151.

Gregory TR. 2019. Animal Genome Size Database, http://www.genomesize.com.

Griffin D, Burt DW. 2014. All chromosomes great and small: 10 years on. *Chromosome Research* **22**: 1-6.

Guiblet WM, Cremona MA, Cechova M, Harris RS, Kejnovská I, Kejnovsky E, Eckert K, Chiaromonte F, Makova KD. 2018. Long-read sequencing technology indicates genome-wide effects of non-B DNA on polymerization speed and error rate. *Genome Research* **28**: 1767-1778.

Harris RS. 2007. Improved pairwise alignment of genomic DNA. *PhD Thesis, The Pennsylvania State University*.

Hartley G, O'Neill RJ. 2019. Centromere Repeats: Hidden Gems of the Genome. *Genes* **10**: 223.

Hobza R, Cegan R, Jesionek W, Kejnovsky E, Vyskot B, Kubat Z. 2017. Impact of Repetitive Elements on the Y Chromosome Formation in Plants. *Genes (Basel)* **8**.

1198 Hron T, Pajer P, Pačes J, Bartůněk P, Elleder D. 2015. Hidden genes in birds. *Genome Biology* **16**:
1199 164.
1200 Hughes AL, Yeager M. 1998. NATURAL SELECTION AT MAJOR HISTOCOMPATIBILITY
1201 COMPLEX LOCI OF VERTEBRATES. *Annual Review of Genetics* **32**: 415-435.
1202 Irestedt M, Jønsson KA, Fjeldså J, Christidis L, Ericson PGP. 2009. An unexpectedly long history of
1203 sexual selection in birds-of-paradise. *BMC Evolutionary Biology* **9**: 235.
1204 Jackman SD, Coombe L, Chu J, Warren RL, Vandervalk BP, Yeo S, Xue Z, Mohamadi H, Bohlmann
1205 J, Jones SJM et al. 2018. Tigmint: correcting assembly errors using linked reads from large
1206 molecules. *BMC Bioinformatics* **19**: 393.
1207 Jain M, Olsen HE, Turner DJ, Stoddart D, Bulazel KV, Paten B, Haussler D, Willard HF, Akeson M,
1208 Miga KH. 2018. Linear assembly of a human centromere on the Y chromosome. *Nature*
1209 *Biotechnology* **36**: 321.
1210 Johnson JM, Edwards S, Shoemaker D, Schadt EE. 2005. Dark matter in the genome: evidence of
1211 widespread transcription detected by microarray tiling experiments. *Trends in Genetics* **21**:
1212 93-102.
1213 Kapitonov VV, Koonin EV. 2015. Evolution of the RAG1-RAG2 locus: both proteins came from the
1214 same transposon. *Biology Direct* **10**: 20.
1215 Kapusta A, Suh A. 2017. Evolution of bird genomes-a transposon's-eye view. *Ann N Y Acad Sci* **1389**:
1216 164-185.
1217 Kozarewa I, Ning Z, Quail MA, Sanders MJ, Berriman M, Turner DJ. 2009. Amplification-free
1218 Illumina sequencing-library preparation facilitates improved mapping and assembly of
1219 (G+C)-biased genomes. *Nat Methods* **6**.
1220 Lajoie BR, Dekker J, Kaplan N. 2015. The Hitchhiker's guide to Hi-C analysis: practical guidelines.
1221 *Methods* **72**: 65-75.
1222 Law JA, Jacobsen SE. 2010. Establishing, maintaining and modifying DNA methylation patterns in
1223 plants and animals. *Nature Reviews Genetics* **11**: 204-220.
1224 Lerat E, Casacuberta J, Chaparro C, Vieira C. 2019. On the Importance to Acknowledge Transposable
1225 Elements in Epigenomic Analyses. *Genes* **10**: 258.
1226 Levin HL, Moran JV. 2011. Dynamic interactions between transposable elements and their hosts.
1227 *Nature Reviews Genetics* **12**: 615-627.
1228 Levis RW, Ganesan R, Houtchens K, Tolar LA, Sheen F-m. 1993. Transposons in place of telomeric
1229 repeats at a Drosophila telomere. *Cell* **75**: 1083-1093.
1230 Li H, Durbin R. 2010. Fast and accurate long-read alignment with Burrows–Wheeler transform.
1231 *Bioinformatics* **26**: 589-595.
1232 Li H, Genome Project Data Processing S, Wysoker A, Handsaker B, Marth G, Abecasis G, Ruan J,
1233 Homer N, Durbin R, Fennell T. 2009. The Sequence Alignment/Map format and SAMtools.
1234 *Bioinformatics* **25**: 2078-2079.
1235 Li Q, Li HB, Huang W, Xu YC, Zhou Q, Wang SH, Ruan J, Huang SW, Zhang Z. 2019. A
1236 chromosome-scale genome assembly of cucumber (Cucumis sativus L.). *Gigascience* **8**: 10.
1237 Lieberman-Aiden E, van Berkum NL, Williams L, Imakaev M, Ragoczy T, Telling A, Amit I, Lajoie
1238 BR, Sabo PJ, Dorschner MO et al. 2009. Comprehensive Mapping of Long-Range
1239 Interactions Reveals Folding Principles of the Human Genome. *Science* **326**: 289-293.
1240 Ligon RA, Diaz CD, Morano JL, Troscianko J, Stevens M, Moskeland A, Laman TG, Scholes E, III.
1241 2018. Evolution of correlated complexity in the radically different courtship signals of birds-
1242 of-paradise. *PLOS Biology* **16**: e2006962.
1243 Loomis EW, Eid JS, Peluso P, Yin J, Hickey L, Rank D, McCalmon S, Hagerman RJ, Tassone F,
1244 Hagerman PJ. 2013. Sequencing the unsequenceable: Expanded CGG-repeat alleles of the
1245 fragile X gene. *Genome Research* **23**: 121-128.
1246 Lowe TM, Eddy SR. 1997. tRNAscan-SE: A Program for Improved Detection of Transfer RNA
1247 Genes in Genomic Sequence. *Nucleic Acids Research* **25**: 955-964.

Marks P, Garcia S, Barrio AM, Belhocine K, Bernate J, Bharadwaj R, Bjornson K, Catalanotti C, Delaney J, Fehr A et al. 2019. Resolving the full spectrum of human genome variation using Linked-Reads. *Genome Research* **29**: 635-645.

McGurk MP, Dion-Côté A-M, Barbash DA. 2019. Rapid evolution at the telomere: transposable element dynamics at an intrinsically unstable locus. *bioRxiv* doi:10.1101/782904: 782904.

Michael TP, Jupe F, Bemm F, Motley ST, Sandoval JP, Lanz C, Loudet O, Weigel D, Ecker JR. 2018. High contiguity Arabidopsis thaliana genome assembly with a single nanopore flow cell. *Nature Communications* **9**: 541.

Miller MM, Taylor RL, Jr. 2016. Brief review of the chicken Major Histocompatibility Complex: the genes, their distribution on chromosome 16, and their contributions to disease resistance. *Poultry Science* **95**: 375-392.

Montoliu-Nerin M, Sánchez-García M, Bergin C, Grabherr M, Ellis B, Kutschera VE, Kierczak M, Johannesson H, Rosling A. 2019. From single nuclei to whole genome assemblies. *bioRxiv* doi:10.1101/625814: 625814.

Nishimura O, Hara Y, Kuraku S. 2017. gVolante for standardizing completeness assessment of genome and transcriptome assemblies. *Bioinformatics* **33**: 3635-3637.

O'Leary NA, Wright MW, Brister JR, Ciufo S, Haddad D, McVeigh R, Rajput B, Robbertse B, Smith-White B, Ako-Adjei D et al. 2015. Reference sequence (RefSeq) database at NCBI: current status, taxonomic expansion, and functional annotation. *Nucleic Acids Research* **44**: D733-D745.

O'Connor EA, Westerdahl H, Burri R, Edwards SV. 2019. Avian MHC Evolution in the Era of Genomics: Phase 1.0. *Cells* **8**: 1152.

Ou S, Chen J, Jiang N. 2018. Assessing genome assembly quality using the LTR Assembly Index (LAI). *Nucleic Acids Research* **46**: e126-e126.

Oyola SO, Otto TD, Gu Y, Maslen G, Manske M, Campino S, Turner DJ, MacInnis B, Kwiatkowski DP, Swerdlow HP et al. 2012. Optimizing illumina next-generation sequencing library preparation for extremely at-biased genomes. *BMC Genomics* **13**: 1.

Paajanen P, Kettleborough G, López-Girona E, Giolai M, Heavens D, Baker D, Lister A, Cugliandolo F, Wilde G, Hein I et al. 2019. A critical comparison of technologies for a plant genome sequencing project. *GigaScience* **8**.

Peñalba JV, Deng Y, Fang Q, Joseph L, Moritz C, Cockburn A. 2019. Genome of an iconic Australian bird: High-quality assembly and linkage map of the superb fairy-wren (*Malurus cyaneus*). *Molecular Ecology Resources* doi:10.1111/1755-0998.13124.

Peona V, Weissensteiner MH, Suh A. 2018. How complete are "complete" genome assemblies?-An avian perspective. *Mol Ecol Resour* doi:10.1111/1755-0998.12933.

Pettersson ME, Rochus CM, Han F, Chen J, Hill J, Wallerman O, Fan G, Hong X, Xu Q, Zhang H et al. 2019. A chromosome-level assembly of the Atlantic herring genome—detection of a supergene and other signals of selection. *Genome Research* doi:10.1101/gr.253435.119.

Platt RN, II, Blanco-Berdugo L, Ray DA. 2016. Accurate Transposable Element Annotation Is Vital When Analyzing New Genome Assemblies. *Genome Biology and Evolution* **8**: 403-410.

Prost S, Armstrong EE, Nylander J, Thomas GWC, Suh A, Petersen B, Dalen L, Benz BW, Blom MPK, Palkopoulou E et al. 2019. Comparative analyses identify genomic features potentially involved in the evolution of birds-of-paradise. *GigaScience* **8**: 1-12.

Putnam NH, O'Connell BL, Stites JC, Rice BJ, Blanchette M, Calef R, Troll CJ, Fields A, Hartley PD, Sugnet CW et al. 2016. Chromosome-scale shotgun assembly using an in vitro method for long-range linkage. *Genome Research* **26**: 342-350.

Quinlan AR. 2014. BEDTools: The Swiss-Army Tool for Genome Feature Analysis. *Current Protocols in Bioinformatics* **47**: 11.12.11-11.12.34.

Raiber E-A, Kranaster R, Lam E, Nikan M, Balasubramanian S. 2011. A non-canonical DNA structure is a binding motif for the transcription factor SP1 in vitro. *Nucleic Acids Research* **40**: 1499-1508.

Rhoads A, Au KF. 2015. PacBio Sequencing and Its Applications. *Genomics, Proteomics & Bioinformatics* **13**: 278-289.

Ribeiro FJ, Przybylski D, Yin S, Sharpe T, Gnerre S, Abouelleil A, Berlin AM, Montmayeur A, Shea TP, Walker BJ et al. 2012. Finished bacterial genomes from shotgun sequence data. *Genome Research* **22**: 2270-2277.

Sahakyan AB, Chambers VS, Marsico G, Santner T, Di Antonio M, Balasubramanian S. 2017. Machine learning model for sequence-driven DNA G-quadruplex formation. *Scientific Reports* **7**: 14535.

Schadt EE, Turner S, Kasarskis A. 2010. A window into third-generation sequencing. *Human Molecular Genetics* **19**: R227-R240.

Schiavone D, Guilbaud G, Murat P, Papadopoulou C, Sarkies P, Prioleau M-N, Balasubramanian S, Sale JE. 2014. Determinants of G quadruplex-induced epigenetic instability in REV1-deficient cells. *The EMBO Journal* **33**: 2507-2520.

Sedlazeck FJ, Lee H, Darby CA, Schatz MC. 2018. Piercing the dark matter: bioinformatics of long-range sequencing and mapping. *Nature Reviews Genetics* **19**: 329-346.

Seo J-S, Rhie A, Kim J, Lee S, Sohn M-H, Kim C-U, Hastie A, Cao H, Yun J-Y, Kim J et al. 2016. De novo assembly and phasing of a Korean human genome. *Nature* **538**: 243.

Shedlock AM, Takahashi K, Okada N. 2004. SINEs of speciation: tracking lineages with retroposons. *Trends Ecol Evol* **19**: 545-553.

Shiina T, Hosomichi K, Inoko H, Kulski JK. 2009. The HLA genomic loci map: expression, interaction, diversity and disease. *Journal Of Human Genetics* **54**: 15.

Slotkin RK. 2018. The case for not masking away repetitive DNA. *Mobile DNA* **9**: 15.

Smeds L, Kawakami T, Burri R, Bolivar P, Husby A, Qvarnström A, Uebbing S, Ellegren H. 2014. Genomic identification and characterization of the pseudoautosomal region in highly differentiated avian sex chromosomes. *Nature Communications* **5**: 5448.

Smeds L, Warmuth V, Bolivar P, Uebbing S, Burri R, Suh A, Nater A, Bureš S, Garamszegi LZ, Hogner S et al. 2015. Evolutionary analysis of the female-specific avian W chromosome. *Nature Communications* **6**: 7330.

Smith JJ, Timoshevskaya N, Timoshevskiy VA, Keinath MC, Hardy D, Voss SR. 2019. A chromosome-scale assembly of the axolotl genome. *Genome Research* **29**: 317-324.

Su X-z, Wu Y, Sifri CD, Wellems TE. 1996. Reduced Extension Temperatures Required for PCR Amplification of Extremely A+T-rich DNA. *Nucleic Acids Research* **24**: 1574-1575.

Suh A, Smeds L, Ellegren H. 2018. Abundant recent activity of retrovirus-like retrotransposons within and among flycatcher species implies a rich source of structural variation in songbird genomes. *Molecular Ecology* **27**: 99-111.

Sun H, Rowan BA, Flood PJ, Brandt R, Fuss J, Hancock AM, Michelmore RW, Huettel B, Schneeberger K. 2019. Linked-read sequencing of gametes allows efficient genome-wide analysis of meiotic recombination. *Nature Communications* **10**: 4310.

Tanaka Y, Asano T, Kanemitsu Y, Goto T, Yoshida Y, Yasuba K, Misawa Y, Nakatani S, Kobata K. 2019. Positional differences of intronic transposons in pAMT affect the pungency level in chili pepper through altered splicing efficiency. *The Plant Journal* **0**.

Thomma BPHJ, Seidl MF, Shi-Kunne X, Cook DE, Bolton MD, van Kan JAL, Faino L. 2016. Mind the gap; seven reasons to close fragmented genome assemblies. *Fungal Genetics and Biology* **90**: 24-30.

Tilak M-K, Botero-Castro F, Galtier N, Nabholz B. 2018. Illumina Library Preparation for Sequencing the GC-Rich Fraction of Heterogeneous Genomic DNA. *Genome Biology and Evolution* **10**: 616-622.

Vertebrate Genome Project V. https://vertebrategenomesproject.org.

Walker BJ, Abeel T, Shea T, Priest M, Abouelliel A, Sakthikumar S, Cuomo CA, Zeng Q, Wortman J, Young SK et al. 2014. Pilon: An Integrated Tool for Comprehensive Microbial Variant Detection and Genome Assembly Improvement. *PLOS ONE* **9**: e112963.

Wallberg A, Bunikis I, Pettersson OV, Mosbech M-B, Childers AK, Evans JD, Mikheyev AS, Robertson HM, Robinson GE, Webster MT. 2019. A hybrid de novo genome assembly of the honeybee, Apis mellifera, with chromosome-length scaffolds. *BMC Genomics* **20**: 275.

Warren RL, Yang C, Vandervalk BP, Behsaz B, Lagman A, Jones SJM, Birol I. 2015. LINKS: Scalable, alignment-free scaffolding of draft genomes with long reads. *GigaScience* **4**: 35.

Warren WC, Hillier LW, Tomlinson C, Minx P, Kremitzki M, Graves T, Markovic C, Bouk N, Pruitt KD, Thibaud-Nissen F et al. 2017. A New Chicken Genome Assembly Provides Insight into Avian Genome Structure. *G3: Genes|Genomes|Genetics* **7**: 109-117.

Waterhouse RM, Seppey M, Simão FA, Manni M, Ioannidis P, Klioutchnikov G, Kriventseva EV, Zdobnov EM. 2017. BUSCO Applications from Quality Assessments to Gene Prediction and Phylogenomics. *Molecular Biology and Evolution* **35**: 543-548.

Watson M, Warr A. 2019. Errors in long-read assemblies can critically affect protein prediction. *Nature Biotechnology* **37**: 124-126.

Weisenfeld NI, Kumar V, Shah P, Church DM, Jaffe DB. 2017. Direct determination of diploid genome sequences. *Genome Res* **27**: 757-767.

Weissensteiner MH, Bunikis I, Catalan A, Francoijs K-J, Knief U, Heim W, Peona V, Pophaly S, Sedlazeck F, Suh A et al. 2019. The population genomics of structural variation in a songbird genus. *bioRxiv* doi:10.1101/830356: 830356.

Weissensteiner MH, Pang AWC, Bunikis I, Hoijer I, Vinnere-Petterson O, Suh A, Wolf JBW. 2017. Combination of short-read, long-read, and optical mapping assemblies reveals large-scale tandem repeat arrays with population genetic implications. *Genome Res* **27**: 697-708.

Weissensteiner MH, Suh A. 2019. Repetitive DNA: The Dark Matter of Avian Genomics. In *Avian Genomics in Ecology and Evolution: From the Lab into the Wild*, doi:10.1007/978-3-030-16477-5_5 (ed. RHS Kraus), pp. 93-150. Springer International Publishing, Cham.

Westbrook CJ, Karl JA, Wiseman RW, Mate S, Koroleva G, Garcia K, Sanchez-Lockhart M, O'Connor DH, Palacios G. 2015. No assembly required: Full-length MHC class I allele discovery by PacBio circular consensus sequencing. *Human Immunology* **76**: 891-896.

Wicker T, Sabot F, Hua-Van A, Bennetzen JL, Capy P, Chalhoub B, Flavell A, Leroy P, Morgante M, Panaud O et al. 2007. A unified classification system for eukaryotic transposable elements. *Nature Reviews Genetics* **8**: 973-982.

Willard HF, Waye JS. 1987. Hierarchical order in chromosome-specific human alpha satellite DNA. *Trends in Genetics* **3**: 192-198.

Wyman SK, Jansen RK, Boore JL. 2004. Automatic annotation of organellar genomes with DOGMA. *Bioinformatics* **20**: 3252-3255.

Xu L, Auer G, Peona V, Suh A, Deng Y, Feng S, Zhang G, Blom MPK, Christidis L, Prost S et al. 2019. Dynamic evolutionary history and gene content of sex chromosomes across diverse songbirds. *Nature Ecology & Evolution* **3**: 834-844.

Yazdi HP, Ellegren H. 2018. A Genetic Map of Ostrich Z Chromosome and the Role of Inversions in Avian Sex Chromosome Evolution. *Genome Biology and Evolution* **10**: 2049-2060.

Yeo S, Coombe L, Warren RL, Chu J, Birol I. 2017. ARCS: scaffolding genome drafts with linked reads. *Bioinformatics* **34**: 725-731.

Yoshimura J, Ichikawa K, Shoura MJ, Artiles KL, Gabdank I, Wahba L, Smith CL, Edgley ML, Rougvie AE, Fire AZ et al. 2019. Recompleting the Caenorhabditis elegans genome. *Genome Research* **29**: 1009-1022.

Zhang G Li C Li Q Li B Larkin DM Lee C Storz JF Antunes A Greenwold MJ Meredith RW et al. 2014. Comparative genomics reveals insights into avian genome evolution and adaptation. *Science* **346**: 1311-1320.

Zhang Y, Cheng TC, Huang G, Lu Q, Surleac MD, Mandell JD, Pontarotti P, Petrescu AJ, Xu A, Xiong Y et al. 2019. Transposon molecular domestication and the evolution of the RAG recombinase. *Nature* **569**: 79-84.

Zheng GXY, Lau BT, Schnall-Levin M, Jarosz M, Bell JM, Hindson CM, Kyriazopoulou-Panagiotopoulou S, Masquelier DA, Merrill L, Terry JM et al. 2016. Haplotyping germline and cancer genomes with high-throughput linked-read sequencing. *Nature Biotechnology* **34**: 303.

Zhou Q, Zhang J, Bachtrog D, An N, Huang Q, Jarvis ED, Gilbert MTP, Zhang G. 2014. Complex evolutionary trajectories of sex chromosomes across bird taxa. *Science* **346**: 1246338.